One-dimensional disordered wires with Pöschl-Teller potentials

Alberto Rodríguez* and Jose M. Cerveró
Física Teórica, Departamento de Física Fundamental, Universidad de Salamanca, 37008 Salamanca, Spain
(Received 11 April 2006; revised manuscript received 4 July 2006; published 5 September 2006)

We study the electronic properties of a one-dimensional disordered chain made up of Pöschl-Teller potentials. The features of the whole spectrum of the random chain in the thermodynamic limit are analyzed in detail by making use of the functional equation formalism. The disordered system exhibits a fractal distribution of states within certain energy intervals and two types of resonances exist for the uncorrelated case. These extended states are characterized by different values of their critical exponents and different behaviors near the critical energies when the system is finite, but their existence can be defined by a single common condition. The chain is also considered including a natural model of short-range correlated disorder. The results show that the effects of the correlations considered are independent of the potential model.

DOI: 10.1103/PhysRevB.74.104201 PACS number(s): 71.23.An, 72.15.Rn, 73.21.Hb

I. INTRODUCTION

The pioneering work of Anderson[1] showed how the electronic properties of a solid can be dramatically affected by the absence of periodicity in the system which gives rise to the spatial localization of the electronic states. Since then the study of disordered systems has been an active area of research and nowadays the physics of disorder constitute a relevant interdisciplinary part of physics whose leading exponent can probably be found in the field of condensed matter. Electronic localization due to disorder is a key element to understanding different physical phenomena such as the quantum Hall effect or the suppression of conductivity in amorphous matter. The effects of disorder are of primary importance in low-dimensional systems: two-dimensional electron gases, one-dimensional quantum wires, etc., whose electronic properties can be seriously affected by the presence of disorder which may indeed yield a very particular phenomenology. During the last few years much has been learnt about the electronic properties of one-dimensional disordered systems. For example, the existence of correlations in the disorder can lead to delocalization and thus improving the transport properties of disordered structures. This has been proved theoretically for short-range correlated disorder which induces the appearance of isolated extended states,[2–14] as well as for long-range correlations that lead to the emergence of a phase of apparently extended states and a qualitative metal-insulator transition.[15–21] These predictions were experimentally confirmed in different systems: semiconductor superlattices[22] and microwave guides,[23,24] respectively. The significance of the appearance of phases of extended states in the spectrum of a disordered system is also increased by the theoretical description of interesting dynamical phenomena such as Bloch oscillations.[25,26] It has also been shown that delocalization in one-dimensional (1D) structures with random disorder can take place due to the existence of long-range interactions.[27–29] On the other hand, universality of the distributions of macroscopic transport-related quantities characterizing disordered systems has been studied by scaling theory (see Ref. 30), which is still evolving nowadays: the conditions for the validity of single parameter scaling (SPS) have been recently reformulated[31,32] and it has been found that different scaling regimes appear when disorder is correlated.[33]

The interest for disorder is also currently registering a noticeable increase in the field of ultracold atomic lattice gases. Optical lattices in one or two dimensions can be used to study the dynamics of Bose-Einstein condensates in the presence of disordered potentials,[34,35] the appearance of Anderson-glass phases in bosonic gases,[36] or the interplay between disorder and interactions.[37] Moreover ultracold atomic gases in optical lattices appear as very favorable systems for the realization of low-dimensional disordered systems and the experimental observation of Anderson localization of matter waves.[38]

In spite of the advance in the understanding of the properties of one-dimensional disordered systems there are several interesting questions which require a deeper study, such as the peculiar features of the distribution of states when disorder appears, whether there exists or not a universal condition for the emergence of extended states in the spectrum, the effects of different models of correlated disorder, or even if it is possible to make a general analytical description of the thermodynamic limit of disordered 1D systems. In order to deepen in some of these problems we study here a one-dimensional random system with a different potential, the Pöschl-Teller potential, which has not been treated in the literature with such a purpose. Some of the characteristic properties of this disordered system have already been reported by the authors.[39] This work is intended to provide a thorough description of the model including a detailed discussion on the conclusions that can be inferred from the results obtained. The paper is organized as follows. In Sec. II the quantum properties of the individual potential are described and in Sec. III we briefly explain the procedure to join several potential units. Section IV is devoted to the study of the properties of uncorrelated disordered chains including features of DOS, appearance of extended states, study of the negative spectrum of energies, etc. The effects of short-range correlations upon this model of potential are described in Sec. V for both infinite and finite chains. Section VI gathers a final discussion on the results and some hypothesis concerning the properties of 1D disordered systems.

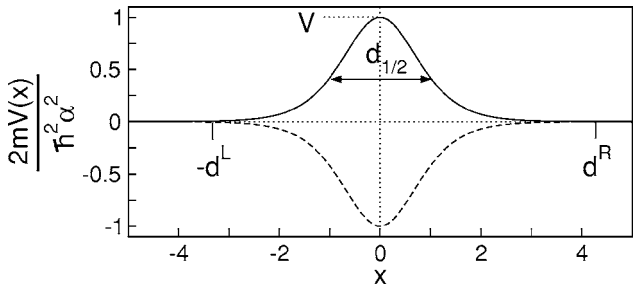

FIG. 1. Pöschl-Teller potential defined in Eq. (1).

II. THE POTENTIAL

Let us consider the general Pöschl-Teller potential, shown in Fig. 1, and given by

$$V(x) = \frac{\hbar^2\alpha^2}{2m}\frac{V}{\cosh^2(\alpha x)}. \tag{1}$$

It resembles the form of an atomic well or barrier depending on the sign of V, a dimensionless parameter that together with α determines the height or depth of the potential. The parameter α, with units of inverse of length, controls the half-width of the potential which reads $d_{1/2}=2\alpha^{-1}\,\mathrm{arccosh}\,\sqrt{2}$. The larger α is, the narrower and higher (deeper) the potential becomes. The Schrödinger equation for the Pöschl-Teller potential is analytically solvable and its solutions are well known.[40–42] Its asymptotic transmission matrix for positive energies reads[43]

$$\mathcal{M} = \begin{pmatrix} e^{i\varphi}\sqrt{1+w^2} & -iw \\ iw & e^{-i\varphi}\sqrt{1+w^2} \end{pmatrix}, \tag{2}$$

where

$$w = \frac{\sin(\pi b)}{\sinh(\pi k/\alpha)}, \quad b = \frac{1}{2} + \sqrt{\frac{1}{4} - V}, \tag{3}$$

$$\varphi = \frac{\pi}{2} + \arg\left\{\frac{\Gamma^2(ik/\alpha)}{\Gamma(b+ik/\alpha)\Gamma(1-b+ik/\alpha)}\right\}, \tag{4}$$

$k=\sqrt{2mE}/\hbar$ and $\Gamma(z)$ is the complex Euler gamma function, w is always a real quantity as can be seen in its alternative definition $w=\cosh(\pi\sqrt{V-1/4})/\sinh(k\pi/\alpha)$. The matrix has the symmetries corresponding to a real and parity invariant potential. The dimensionless amplitude in terms of b reads $V=-b(b-1)$ which is the usual form found in the literature. Let us remark that the above expressions are only valid for positive energies since several simplifications have been carried out with the assumption of $k\in\mathbb{R}$. From Eq. (2) the asymptotic probability of transmission is $T=(1+w^2)^{-1}$. One characteristic feature of this potential is that $T=1$ for all energies whenever b is a real integer. Hence an absolute resonant transmission occurs for potential wells with $V=-2$, $-6,-12,-20,\ldots$, independently of the value of α.

In the case of potential wells ($V<0$) several bound states exist, that can be calculated from the poles of the transmission amplitude by making a proper extension into the complex plane via $k\to i\eta$, where η can be considered to be positive without loss of generality. The correct form of the transmission matrix for negative energies reads

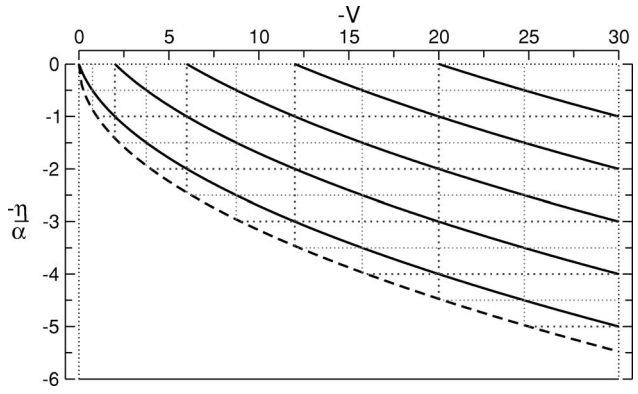

FIG. 2. Bound states for the Pöschl-Teller well. The solid curves mark the position of the eigenstates given by Eq. (8). The dashed line mark the position of the bottom of the well ($-\sqrt{|V|}$). The dotted grids highlight the integer and the half-integer states.

$$\mathcal{M} = \begin{pmatrix} f(-\eta) & -q \\ q & f(\eta) \end{pmatrix}, \tag{5}$$

where

$$q = \frac{\sin(\pi b)}{\sin(\pi\eta/\alpha)}, \tag{6}$$

$$f(\eta) = \frac{\eta/\alpha\Gamma^2(\eta/\alpha)}{\Gamma(1-b+\eta/\alpha)\Gamma(b+\eta/\alpha)}. \tag{7}$$

The condition for bound states is then $f(\eta)=0$. Since for potential wells b is real and greater than 1 the eigenstate equation reduces to $\Gamma^{-1}(1-b+\eta/\alpha)=0$, which is satisfied whenever the argument of the gamma function equals a negative integer or zero. Finally, the energies of the bound states are

$$\frac{\eta}{\alpha} = b - m, \quad m = 1,2,3,\ldots,[b], \tag{8}$$

where $[b]$ reads the integer part of b. Therefore the Pöschl-Teller well host in general $[b]$ bound states equally spaced in the variable $\eta=\sqrt{2m|E|}/\hbar$ (Fig. 2), except for resonant wells which host $b-1$ bound states. A couple of peculiar cases deserve comment.

(1) If b is an integer then the energies of the bound states are also integers. $\eta/\alpha=m$, $m=1,2,\ldots,b-1$. This is also the case for which the potential well behaves as an absolute transparent potential for all energies (resonant well). Example values for the dimensionless amplitude $V=-2,-6,-12,-20,-30,\ldots$.

(2) If b is a half integer then the energies of the bound states are also half integers. $\eta/\alpha=m+1/2$, $m=0,1,\ldots,b-3/2$. In this case the transmission takes the form $T=\tanh^2(\pi k/\alpha)$ independently of b. Some values of the dimensionless amplitude for this situation are $V=-0.75,-3.75,-8.75,-15.75,-24.75,\ldots$.

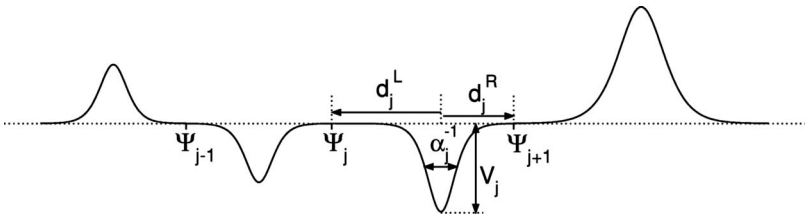

FIG. 3. Potential of a disordered Pöschl-Teller wire.

We shall see how due to the characteristic features exhibited by the Pöschl-Teller potential some exciting effects arise when several potential units are connected.

III. BUILDING LINEAR CHAINS

To build a chain with the potentials described, one must do the approximation of considering that each potential unit has a finite range. Hence a cutoff must be included in the Pöschl-Teller potential. Using this approximation one obtains matrices suitable to be composed in linear chains. Let us suppose that the potential is appreciable only inside the interval $[-d^L, d^R]$, where the superindices L, R, stand for the left and right lengths of the interval from the center of the potential (Fig. 1). Outside this interval the wave function is assumed to be a superposition of the free particle solutions. After some algebra one finds that the transmission matrix for the cutoff potential reads[44,45]

$$\mathbf{M}_{\text{cut}} = \begin{pmatrix} e^{i[\varphi+k(d^R+d^L)]}\sqrt{1+w^2} & -iwe^{ik(d^R-d^L)} \\ iwe^{-ik(d^R-d^L)} & e^{-i[\varphi+k(d^R+d^L)]}\sqrt{1+w^2} \end{pmatrix}. \tag{9}$$

The cutoff matrix is the same as the asymptotic one plus an extra phase term in the diagonal elements that accounts for the total distance (d^R+d^L) during which the particle feels the effect of the potential, and also an extra phase term in the off-diagonal elements measuring the asymmetry of the cutoff (d^R-d^L). These phases are the key quantities since they will be responsible of the interference processes that produce the transmission patterns. The goodness of this procedure depends on the decay of the potential. In our case due to the rapid decay of the Pöschl-Teller potential the cutoff distance admits very reasonable values. In fact we have seen that for a sensible wide range of the parameters α and V, one can take as a minimum value for the cutoff distance $d_0=2d_{1/2} \simeq 3.5/\alpha$, where $d_{1/2}$ is the half-width. Taking $d^{L,R} \geqslant d_0$ the connection procedure of potentials works really well, as we have checked in several cases comparing the analytical composition of matrices versus a numerical integration of the Schrödinger equation for the global potential. The above matrix can be used to study analytically and numerically the scattering process of different Pöschl-Teller composite potential profiles.[43]

IV. WIRES WITH UNCORRELATED DISORDER

Once the properties of the potential have been studied and the procedure for constructing linear arrays has been described, let us consider now the effects of uncorrelated disorder upon this particular model. First is obtaining the canonical equation applying to the electronic states inside the system. From the transmission matrix (9) one is led to the following relation:[44,45]

$$\Psi_{j+1} = \left(\bar{S}_j + S_{j-1}\frac{K_j}{K_{j-1}}\right)\Psi_j - \frac{K_j}{K_{j-1}}\Psi_{j-1}, \tag{10}$$

where

$$\bar{S}_j = -w_j \sin[k(d_j^L - d_j^R)] + \sqrt{1+w_j^2}\cos(\Phi_j), \tag{11}$$

$$S_j = w_j \sin[k(d_j^L - d_j^R)] + \sqrt{1+w_j^2}\cos(\Phi_j), \tag{12}$$

$$K_j = w_j \cos[k(d_j^L - d_j^R)] + \sqrt{1+w_j^2}\sin(\Phi_j), \tag{13}$$

in terms of w and φ defined in Eqs. (3) and (4) and $\Phi_j = k(d_j^L+d_j^R)+\varphi_j$. The amplitudes Ψ_j correspond to the value of the state at the junction points of the potentials as shown in Fig. 3, and in this case each potential is determined by four parameters $d_j^L, d_j^R, \alpha_j, V_j$. For negative energies the canonical equation reads the same but the functions must be defined as

$$\bar{S}_j = -q_j \sinh[\eta(d_j^L - d_j^R)] + \frac{1}{2}[e^{\eta(d_j^L+d_j^R)}f_j(\eta) + e^{-\eta(d_j^L+d_j^R)}f_j(-\eta)], \tag{14}$$

$$S_j = q_j \sinh[\eta(d_j^L - d_j^R)] + \frac{1}{2}[e^{\eta(d_j^L+d_j^R)}f_j(\eta) + e^{-\eta(d_j^L+d_j^R)}f_j(-\eta)], \tag{15}$$

$$K_j = q_j \cosh[\eta(d_j^L - d_j^R)] + \frac{1}{2}[e^{-\eta(d_j^L+d_j^R)}f_j(-\eta) - e^{\eta(d_j^L+d_j^R)}f_j(\eta)], \tag{16}$$

in terms of q and $f(\eta)$ defined in Eqs. (6) and (7). The canonical equation functions adopt a simpler form if the cutoff of the potentials is chosen to be symmetric and in this case $\bar{S}_j = S_j$.

The properties of the uncorrelated disordered chain in the thermodynamic limit, composed by different species with parameters $\{\mathbf{v}_\gamma \equiv (d_\gamma^L, d_\gamma^R, \alpha_\gamma, V_\gamma)\}$ and concentrations $\{c_\gamma\}$ are obtained from the functional equation formalism which is thoroughly explained in Refs. 44 and 45. Let us make a brief description for this model. One needs to solve the following set of functional equations:

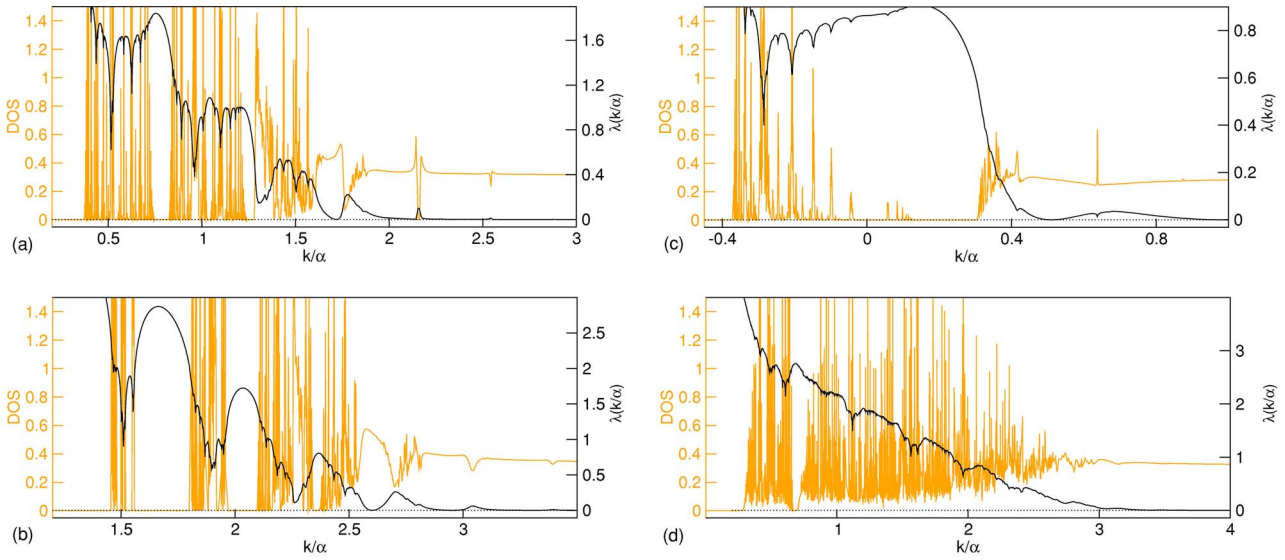

FIG. 4. (Color online) DOS and Lyapunov exponent (black) for several disordered Pöschl-Teller wires with parameters (a) $V_\gamma[c_\gamma]$: −4[0.5], 3[0.5], (b) $V_\gamma[c_\gamma]$: 5[0.5], 7[0.5], (c) $V_\gamma[c_\gamma]$: −1[0.5], −3[0.5], and (d) $V_\gamma[c_\gamma]$: 1[0.2], 6[0.2], −5[0.2], −1[0.2], 9[0.2]. Notice the different vertical scales for DOS (left) and λ (right). The negative part of the abscissa axis represents negative energies $(-\eta/\alpha)$.

$$W_\gamma(\theta) = \sum_\beta c_\beta \left| W_\beta[\mathcal{T}^{-1}(\theta;\mathbf{v}_\beta,\mathbf{v}_\gamma)] - W_\beta\left(\frac{\pi}{2}\right) + \delta(\mathbf{v}_\beta,\mathbf{v}_\gamma) \right|, \tag{17a}$$

$$W_\gamma(\theta + n\pi) = W_\gamma(\theta) + n, \quad \theta \in [0,\pi), n \in \mathbb{Z}, \tag{17b}$$

where the subindices γ,β runs over all species, $\delta(\mathbf{v}_\beta,\mathbf{v}_\gamma) = 1$ if $[K(\mathbf{v}_\beta)/K(\mathbf{v}_\gamma)] > 0$ and $\delta(\mathbf{v}_\beta,\mathbf{v}_\gamma) = 0$ otherwise, and

$$\mathcal{T}^{-1}(\theta;\mathbf{v}_\beta,\mathbf{v}_\gamma) \equiv \arctan\left\{ \frac{K(\mathbf{v}_\beta)}{K(\mathbf{v}_\gamma)} \left(J(\mathbf{v}_\beta,\mathbf{v}_\gamma) - \frac{1}{\tan\theta} \right) \right\}, \tag{18}$$

with $J(\mathbf{v}_\beta,\mathbf{v}_\gamma) = \bar{S}(\mathbf{v}_\gamma) + S(\mathbf{v}_\beta)K(\mathbf{v}_\gamma)/K(\mathbf{v}_\beta)$, where $\bar{S}$, S, and K are the functions of the canonical equation. From the solutions $\{W_\gamma(\theta)\}$ of the functional equations one can obtain the Lyapunov exponent and the DOS of the disordered system in the thermodynamic limit. The inverse of the localization length comes from

$$\lambda(\epsilon) = \frac{1}{2}\sum_{\gamma,\beta} c_\gamma c_\beta \int_0^\pi dW_\gamma(\theta) \ln \mathcal{F}(\theta;\mathbf{v}_\gamma,\mathbf{v}_\beta), \tag{19}$$

where $\epsilon \equiv k/\alpha$ is a dimensionless representation of the energy, α is a reference value for the parameters α_γ, and

$$\mathcal{F}(\theta;\mathbf{v}_\gamma,\mathbf{v}_\beta) \equiv \cos^2\theta + \left(J(\mathbf{v}_\gamma,\mathbf{v}_\beta)\cos\theta - \frac{K(\mathbf{v}_\beta)}{K(\mathbf{v}_\gamma)}\sin\theta \right)^2. \tag{20}$$

And the DOS in the thermodynamic limit per piece of length α^{-1} reads

$$g(\epsilon) = \left| \sum_\gamma \frac{(\alpha_\gamma/\alpha)}{\alpha_\gamma(d_\gamma^L + d_\gamma^R)} \operatorname{sgn}[K(\mathbf{v}_\gamma)] c_\gamma \frac{dW_\gamma\left(\frac{\pi}{2}\right)}{d\epsilon} \right|. \tag{21}$$

The functional equations are solved numerically for each value of the energy, then the localization length and the distribution of states can be obtained using definitions (19) and (21). On the one hand, the fact that the potentials are determined by four independent parameters gives a high degree of versatility to the model, but on the other hand specifying the configuration of the disordered wire including several species can be really a tedious and repetitive task since one needs to list a large amount of parameters. Therefore, from now on whenever the only configurational parameters of a chain are the dimensionless amplitudes $\{V_\gamma\}$, it is implied that $\alpha_\gamma = \alpha$ for all species included in the chain and also that the cutoff is symmetric and its distance is set to $d = 4/\alpha$, so that the total length of every potential is $2d = 8/\alpha$. Several examples of distributions of states and Lyapunov exponents in the thermodynamic limit for different Pöschl-Teller disordered wires can be seen in Fig. 4.

A. General features of the DOS

In the examples given in Fig. 4 the salient features of the distribution of states for this model can be observed. As must be expected, whenever potential wells are included in the disordered chain a group of permitted levels appears for negative energies, which correspond to bound states of the global composite potential. For positive high energies the correct asymptotic value of the free particle distribution is reached in all cases [it can be easily checked that the asymptotic value is $g_{\text{free}}(\epsilon) = \pi^{-1}$]. As with other one-dimensional models,[45,46] for the Pöschl-Teller disordered wires the density of states in the thermodynamic limit also

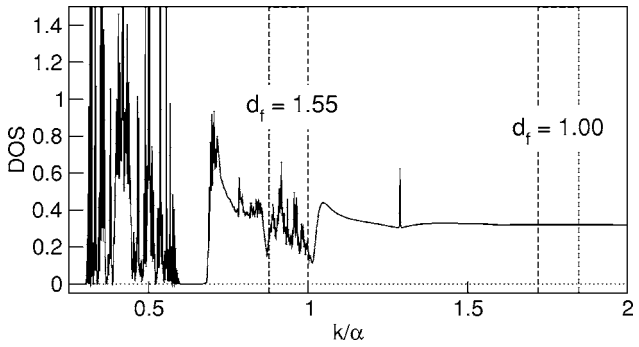

FIG. 5. DOS for a binary disordered Pöschl-Teller wire with parameters $V_1=1$ and $V_2=-1$ and equal concentrations. d_f indicates the fractal dimension of the portion of the DOS contained between the dashed lines.

shows an irregular fluctuating behavior in certain energy ranges. The peaky structure lies almost entirely in the energy range below the maximum height of the potential barriers constituting the array. When the energy goes over the top of the potential barriers $[\epsilon \geqslant (\alpha_\gamma/\alpha)\sqrt{V_\gamma}]$, the carriers found a regular distribution of states that evolves smoothly towards the value π^{-1} as the energy grows. This description agrees with the intuitive reasoning that for energies exceeding the barriers the effects of the potential and hence of the disorder must drastically decrease. In the cases when the system contains only potential wells, the DOS is regular for almost all the positive spectrum [Fig. 4(c)] and the asymptotic value $g_{\text{free}}(\epsilon)$ is reached for very low energies. The structure of the positive spectrum is naturally much more complex when the chain includes potential barriers. Regarding the sharp-pointed structure, we are led to the conclusion that the DOS lacks differentiability at all points within this irregular regions. In fact several analysis can be performed on the distribution of states yielding the conclusion that the density of states for the disordered Pöschl-Teller wires in the thermodynamic limit exhibits a fractal behavior in certain energy ranges. We have been able to quantify numerically the fractal dimension of the distribution. For the binary wire considered in Fig. 5 the analysis yields a fractal dimension $d_f=1.5526$ in the interval $\epsilon \in [0.88, 1]$ and $d_f=1.0038$ for the smooth interval $\epsilon \in [1.72, 1.85]$ where the fractal dimension tends to equate the topological dimension of a curve. This fractal behavior is apparently a consequence of the presence of disorder and it seems to occur in other one-dimensional models as well.[46] A thorough study on this interesting feature of the distribution of states and its relation with the type of disorder will be reported elsewhere.[47]

B. Electronic localization

Let us have a look at the electronic localization for this disordered model. From what can be seen in Figs. 4 and 5 the Lyapunov exponent registers globally the localization of the electronic states. As expected, the localization length increases with the energy. When potential barriers are included in the chain, it can be noticed how for energies above the maximum barrier height the electrons become strongly delocalized. If the wire is composed only of potential wells, the Lyapunov exponent takes very low values for almost all the permitted positive spectrum. As can be seen in the examples given, the Lyapunov exponent tends to decrease in the peaks of the DOS and increase in the troughs. It seems that the state is less localized when it lies on a range containing a large number of permitted levels close to its energy, whereas on the contrary an isolated energy shows always a stronger localization. Let us remark that localization is always weaker inside the nonfractal regions of the spectrum, whereas fractality of the distribution of states seems to be linked to a strong localization. The most important feature concerning the electronic localization is the presence of isolated energies for which the Lyapunov exponent vanishes (Fig. 4). These critical energies are always located inside nonfractal regions of the spectrum, they appear apparently only for binary chains and their values depend on the compositional species. Before going into a detailed analysis, let us remark that the localization properties deduced from the behavior of the Lyapunov exponent are also faithfully confirmed by the inverse participation ratio (IPR) calculated for finite chains after averaging over several realizations of the disordered sequences (Fig. 6). The IPR is defined in terms of the amplitudes of the electronic state at the different sites of the system as

$$\text{IPR} = \frac{\sum_{j=1}^{N} |\Psi_j|^4}{\left(\sum_{j=1}^{N} |\Psi_j|^2\right)^2}. \tag{22}$$

For an extended state the IPR takes values of order N^{-1} whereas for a state localized in the vicinity of only one site it goes to 1. The inverse of the IPR means the length of the portion of the system in which the amplitudes of the states differ appreciably from zero.

The isolated resonances of the spectrum seem to be independent of the concentrations of the binary chains, as can be seen in Fig. 7, where the evolution of the Lyapunov exponent with the concentration of the disordered wire is shown. Let us notice that when the chain is partially or totally composed of potential barriers the resonances can occur for energies below or above the maximum barrier height as can be checked in the different examples given. Around every resonance there exists a range of energies in which the Lyapunov exponent takes very low values and the higher the energy of the resonance the wider this interval is. In fact, the number of resonances may be infinite but above a certain energy they are indistinguishable since the Lyapunov exponent is almost zero anyway.

The appearance of the extended states shown in the examples given can be explained by the arguments given by Gómez and co-workers for a square barrier model,[48] based on the commutativity of the product of the individual transmission matrices of the system, that we shall review here. In the case of a binary chain composed of matrices $\mathbf{M}_1, \mathbf{M}_2$, critical energies ϵ_c can be found among those that satisfy $[\mathbf{M}_1, \mathbf{M}_2]=0$. This is a necessary condition but not a suffi-

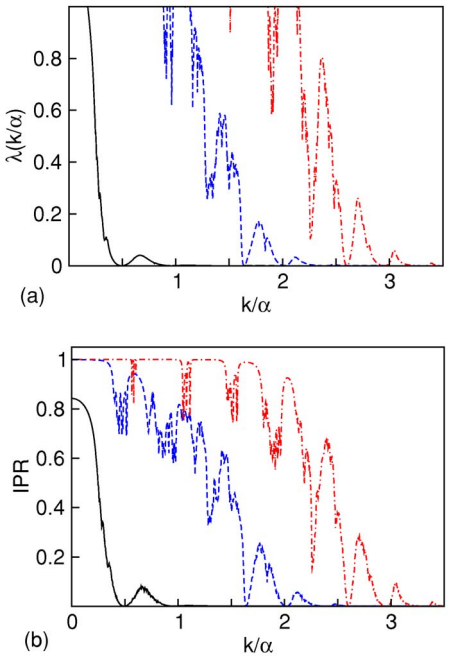

FIG. 6. (Color online) Comparison of Lyapunov exponent (a) and IPR (b) as functions of the energy, for different binary disordered chains. The parameters for the different chains are $V_\gamma[c_\gamma]$: $-1.5[0.5]$, $-4[0.5]$ (solid), $1[0.5]$, $3[0.5]$ (dash), $5[0.5]$, $7[0.5]$ (dash-dot). The IPR is obtained averaging over 100 realizations of a 1000-atom array.

cient one. Now since for these energy values the matrices of the two species commute, the disordered sequence can be changed at will and therefore the effects of the disorder disappear. Let us imagine that the atoms are rearranged so that the sequence becomes a juxtaposition of two semi-infinite pure chains. It is clear that the transparency intervals common to both pure chains are also transparent. Therefore if ϵ_c lies on the permitted bands of both species pure chains it will be a resonance of transmission and an extended state in the thermodynamic limit. Let us remark that this reasoning holds for all values of the concentrations in the binary array. To summarize, in a binary disordered system extended states exist at energies ϵ_c fulfilling the following requirements: commutative matrix product ($[\mathbf{M}_1,\mathbf{M}_2]=0$), and they belong to the permitted spectrum of both species. For the Pöschl-Teller model the commutator of the transmission matrices in the more general case reads

$$[\mathbf{M}_1,\mathbf{M}_2] = \begin{pmatrix} y & z \\ z^* & y^* \end{pmatrix}, \tag{23}$$

where

$$y = -2iw_1w_2 \sin[k(d_1^L - d_1^R - d_2^L + d_2^R)], \tag{24}$$

$$z = 2e^{ik(d_2^R - d_2^L)}w_2\sqrt{1+w_1^2}\sin[k(d_1^L + d_1^R) + \varphi_1] - 2e^{ik(d_1^R - d_1^L)}w_1\sqrt{1+w_2^2}\sin[k(d_2^L + d_2^R) + \varphi_2], \tag{25}$$

that for the critical energies must be zero. And the condition of belonging to the permitted spectrum of the pure chains

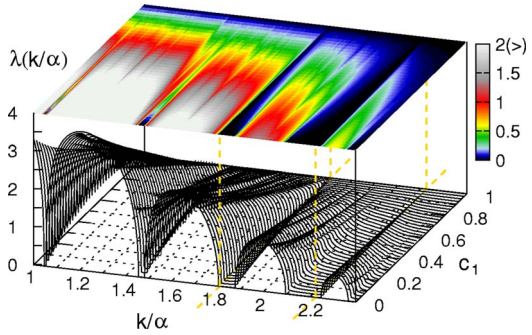

FIG. 7. (Color online) Evolution of the Lyapunov exponent vs energy and concentration for disordered binary wires with parameters $V_1=-2.5$, $V_2=5$. Resonances occur at $\epsilon_c=1.809$, $\epsilon_c=2.226$. The top mapping shows the Lyapunov exponent in a color scale. Notice how the resonances are present for all concentrations.

can straightforwardly be written from the trace of the transmission matrix

$$|\sqrt{1+w_j^2}\cos[k(d_j^L + d_j^R) + \varphi_j]| \leqslant 1, \quad j = 1,2. \tag{26}$$

In the case of symmetric potentials with the same α, the commutator can be written in a very simple form and seemingly for all values of the dimensionless amplitudes V_1, V_2 there exist critical energies, similar to the ones observed in Figs. 4, 6, and 7. For asymmetric species with different α it is also possible to find extended states very easily without doing awkward or very restrictive fits of the parameters (Fig. 8). This kind of resonance, that we shall refer to as commuting resonances (according to Ref. 48), appear very often and they are very versatile in the sense that their presence seem to be compatible with a wide continuous range of several parameters of the potentials.

Finally in the case of a binary chain in which the eight parameters of the system (four for each species) are chosen freely, one would expect in principle to see no resonances in the spectrum, since in this case it will be more difficult to satisfy all requirements for a critical energy to exist. In this situation one can still find several energies for which the Lyapunov exponent takes very low values although it does not vanish completely. An example can be seen in Fig. 9. This behavior happens at energies for which the resonance condition is close to be satisfied, i.e., the commutator of the transmission matrices is relatively small and the energy lies near or in the common permitted spectrum of both species. This fact can be clearly observed in Fig. 9 where the Lyapunov exponent is plotted together with the Euclidean norm of the commutator of the transmission matrices $\|[\mathbf{M}_1,\mathbf{M}_2]\|$. The $\lambda(\epsilon)$ decreases strongly near the minima of the norm of the commutator. This kind of energies appears surprisingly very often when choosing the parameters of the binary system freely, and that is due to the nature of the elements of the commutator. The functions y, $\mathrm{Re}(z)$ and $\mathrm{Im}(z)$ are oscillatory functions whose amplitude decay with the energy, hence even when choosing all the parameters of the chain at random there exist always some energy intervals within which all the functions crosses zero relatively near from one another. It is remarkable the fact that inside the

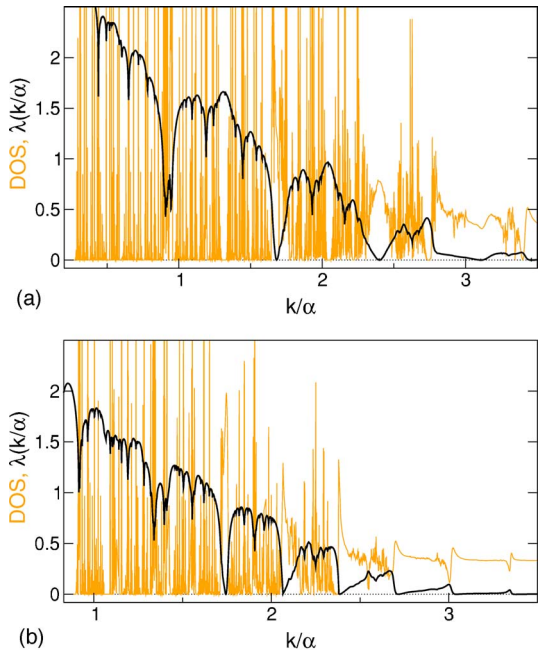

FIG. 8. (Color online) DOS and Lyapunov exponent (black) for binary chains. (a) Two species with symmetric cutoff: $\alpha_1=\alpha$, $V_1=-1$, $d_1=4.5/\alpha_1$ and $\alpha_2=1.95\alpha$, $V_2=2$, $d_2=4.1/\alpha_2$. The three first resonances occur at $\epsilon_c=1.6818$, $\epsilon_c=2.3986$, and $\epsilon_c=3.1064$. Notice that the first two resonances are located below the barrier height $\epsilon_{\max}=1.95\sqrt{2}\simeq 2.76$. (b) Two species with asymmetric cutoff: $\alpha_1=\alpha$, $V_1=1$, $d_1^L=5.2/\alpha_1$, $d_1^R=4.2/\alpha_1$ and $\alpha_2=1.5\alpha$, $V_2=3$, $d_2^L=6.8/\alpha_2$, $d_2^R=5.3/\alpha_2$. The first four resonances occur at $\epsilon_c=1.7434$, $\epsilon_c=2.0618$, $\epsilon_c=2.3865$, and $\epsilon_c=2.7143$. Notice that the first three resonances are located below the highest barrier $\epsilon_{\max}=1.5\sqrt{3}\simeq 2.60$.

common permitted spectrum of both species the norm of the commutator as a function of the energy describes qualitatively the behavior of the Lyapunov exponent. It seems that a strong contribution to the localization length could come from the commutator of the transmission matrices. To quantify this contribution it would be necessary to deepen in the physical meaning of the commutator within this context, but this task surely requires a more profound analysis.

Commuting resonances naturally emerge for a binary system but they could also be found in ternary and higher chains. In fact we have done so for a ternary chain, although the fit of the parameters is much more restrictive as N grows in comparison with the binary case. For N species all the binary commutators must vanish and at the same time the energies must belong to the permitted spectrum of all species. In the Pöschl-Teller model there exists an upper bound for the number of species to find commuting resonances, since the equations of resonance condition grows quadratically with N and the number of variables (parameters of the potential) does linearly.

Extended states can also appear in the thermodynamic limit of disordered systems by imposing different conditions in principle, such as, for example, the one introduced by Hilke and Flores to describe extended states in a square barrier/well model.[49] The condition consists in imposing $\Psi_{j+1}=\pm\Psi_j$ for all sites of the system. Clearly if all species of

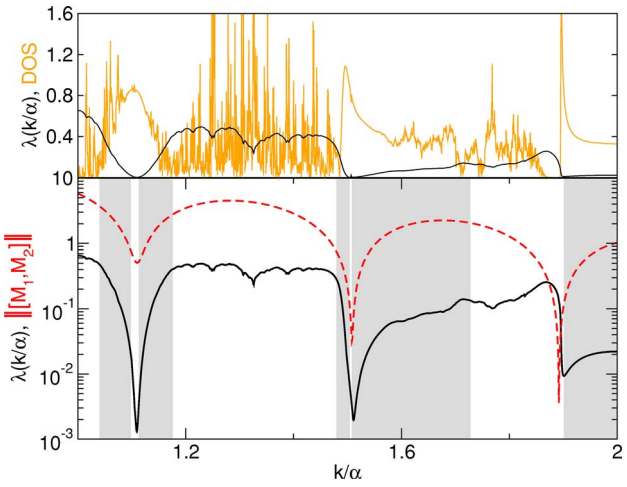

FIG. 9. (Color online) Lyapunov exponent (solid line) for a binary chain with random parameters $\alpha_1=\alpha$, $V_1=-4$, $d_1^L=4/\alpha_1$, $d_1^R=5/\alpha_1$ and $\alpha_2=1.8\alpha$, $V_2=1$, $d_2^L=6/\alpha_2$, $d_2^R=4.5/\alpha_2$. The dashed line corresponds to the Euclidean norm of the commutator of the transmission matrices. Shaded zones highlight the common permitted spectrum of both species. The upper box combines density of states and Lyapunov exponent.

the chain satisfy this constraint for the same energy a transmission resonance arises in the thermodynamic limit. Our Pöschl-Teller disordered wires can also host extended states of this kind. Let us see how one can build them by imposing the specific conditions to the transmission matrices of the individual species included in the system. Let us consider the transmission matrix of a real potential ranging in the interval $[x_j,x_{j+1}]$. Its transfer matrix is an element of the group SU(1,1) and it connects the amplitudes of the traveling plane waves $e^{\pm ikx}$ on both sides of the potential (A_j,B_j) and (A_{j+1},B_{j+1}). The coordinates are chosen to ensure that the state right before the potential Ψ_j, and right after the potential Ψ_{j+1}, is simply given by the sum of the respective complex amplitudes. Then, one can wonder about the form the transmission matrix must adopt to satisfy the condition $\Psi_{j+1}=\pm\Psi_j$. It can be easily calculated that the transmission matrix must fit the expression

$$\mathbf{M}=\begin{pmatrix}\pm 1-ia & -ia\\ ia & \pm 1+ia\end{pmatrix},\quad a\in\mathbb{R}. \tag{27}$$

Thus whenever the transmission matrix takes this form, the probability distribution of the state does not decay after the individual potential but it remains constant. Trivially, the matrices (27) constitute a subgroup of SU(1,1). Then a disordered linear array of potentials which can be described in terms of these matrices will give rise to a completely extended state with a flat probability distribution. Imposing the given form to the most general transmission matrix for a real potential

$$\mathbf{M}_j=\begin{pmatrix}\Lambda_j & \beta_j\\ \beta_j^* & \Lambda_j^*\end{pmatrix},\quad |\Lambda_j|^2-|\beta_j|^2=1, \tag{28}$$

one is led to equations

$$\mathrm{Im}(\Lambda_j) = \mathrm{Im}(\beta_j), \tag{29a}$$

$$\mathrm{Re}(\beta_j) = 0, \quad \forall\, j, \tag{29b}$$

and they straightforwardly guarantee that $\mathrm{Re}(\Lambda_j) = \pm 1$. This latter condition implies that the energy is a common band edge of the periodic spectrum of all species. Therefore, this kind of extended state corresponds to a certain class of common band edges of the spectrum of the individual species composing the wire. If the individual potentials are symmetric the above conditions are simplified since Eq. (29b) is identically satisfied. Notice, however, that not all common band edges of symmetric potentials will be resonances since Eq. (29a) needs to be fulfilled.

Now in the case of a disordered binary Pöschl-Teller wire, one could choose the values of the parameters of the potentials so that there exists an energy ϵ_c for which the matrices of both species take the form (27). From Eq. (9) it follows that the conditions for ϵ_c to exist are

$$\sqrt{1+w_j^2}\,\sin[k(d_j^R + d_j^L) + \varphi_j] = -\,w_j \cos[k(d_j^R - d_j^L)], \tag{30a}$$

$$w_j \sin[k(d_j^R - d_j^L)] = 0, \quad j = 1,2. \tag{30b}$$

For the sake of clarity let us restrict to the default case of symmetric cutoff $d = 4/\alpha$, and the same α for both species. In this case the only constraint is

$$\sqrt{1+w_j^2}\,\sin(8\epsilon_c + \varphi_j) + w_j = 0, \quad j = 1,2, \tag{31}$$

or $K_j = 0$, using the canonical equation function (13). Therefore for a fixed V_1 one chooses one of the infinite roots of $K_1(\epsilon)$ to place the extended state, namely ϵ_c, and then equation $K_2(\epsilon_c) = 0$ is solved in terms of V_2. In some cases several solutions exist for the latter equation. Then the Lyapunov exponent will vanish at ϵ_c for the disordered binary chain independently of the concentrations. A couple of examples are shown in Fig. 10 where the Lyapunov exponent for two binary chains is plotted. Notice that the existence of this kind of extended states is compatible with the presence of commuting-resonances. In fact matrices (27) constitute an abelian subgroup of SU(1,1) as can be straightforwardly checked, which means that the resonances arising from the common band edges are in fact particular cases of commuting-resonances arising from a very precise fit of the parameters of the different species. These extended states are exactly of the same type as the π resonances for the delta model with substitutional disorder,[46] since for the multiples of π the matrices for the delta potential commute with each other independently of the potential coupling, and these energies are always band edges of the periodic delta chain independently of the delta coupling. Although these critical energies are also commuting resonances we shall refer to them using a different label, let us call them CBE resonances (common band-edge resonances). The CBE resonances and the rest of commuting-resonances exhibit very different features as we shall see.

Let us check the functional dependence of the Lyapunov exponent and the density of states near the resonant energies.

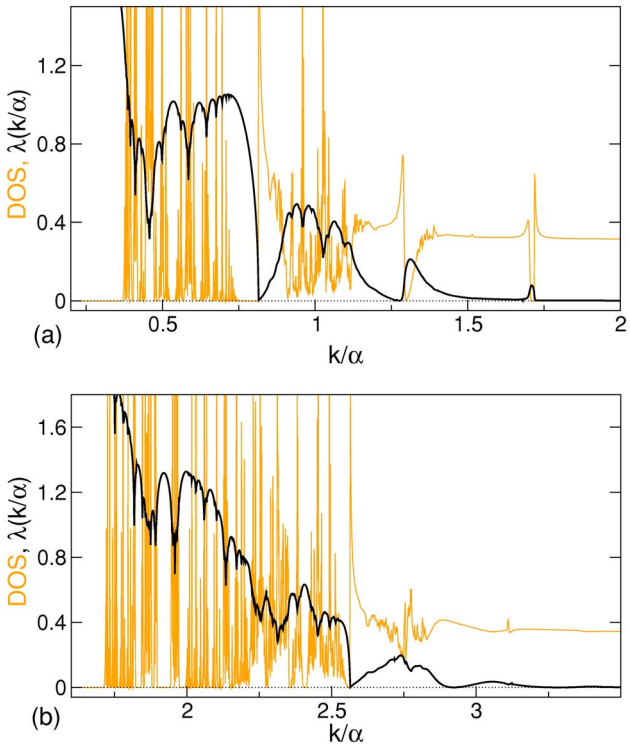

FIG. 10. (Color online) DOS and Lyapunov exponent (black) for binary chains with parameters (a) $V_1 = -4$, $V_2 = 1.571051$ and (b) $V_1 = 4$, $V_2 = 7.217957$ with equal concentrations in both cases. The CBE resonances are located at $\epsilon_c = 0.814459$ and $\epsilon_c = 2.56389$, respectively.

In the case of CBE resonances a careful inspection reveals an asymmetric behavior of the Lyapunov exponent around the critical energy. Seemingly it can be well described by

$$\lambda(\epsilon) \sim \begin{cases} |\epsilon - \epsilon_c|, \\ |\epsilon - \epsilon_c|^{1/2}, \end{cases} \tag{32}$$

on the different sides, as can be observed in Fig. 11(a). The DOS apparently behaves in the same way as for a periodic chain near a band edge: gap on the side where the critical exponent for $\lambda(\epsilon)$ is $1/2$ and dependence of the type $g(\epsilon) \sim |\epsilon - \epsilon_c|^{-1/2}$ on the side with the linear change of the Lyapunov exponent. The behavior near the CBE resonances is apparently the same as for the π resonances in most of the delta chains.[45,50] These resonances seem to exhibit similar features independently of the potential model. From the dependence of the DOS and the localization length near the critical energy, it straightforwardly follows that the number of states around the CBE resonance whose localization length is larger than the system size, in a finite chain, scales as $\sqrt{N}$ where N is the number of atoms.

On the other hand the behavior of the distribution of states and the localization length in the vicinity of a general commuting-resonance is completely different. In all cases studied the Lyapunov exponent seems to fit a quadratic dependence around the critical energy $\lambda(\epsilon) \sim (\epsilon - \epsilon_c)^2$, where the coefficients for $\epsilon < \epsilon_c$ and $\epsilon > \epsilon_c$ can differ. The DOS around these resonances evolves linearly $g(\epsilon) \sim g_0 + (\epsilon - \epsilon_c)$.

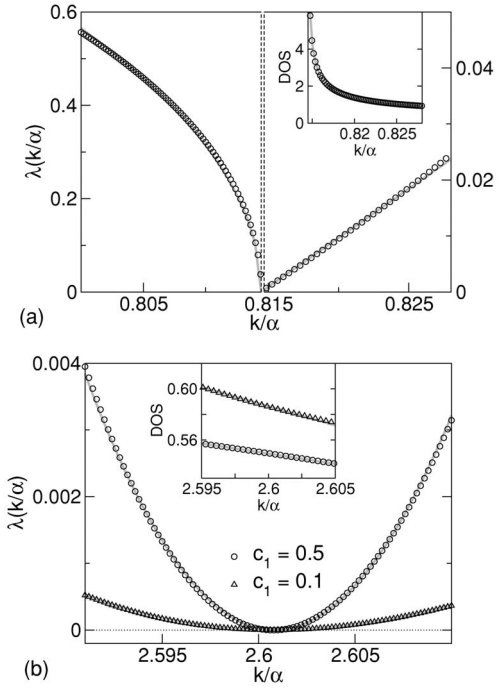

FIG. 11. Behavior of DOS and Lyapunov exponent near critical energies for binary wires. Symbols mark numerical results. (a) $V_1=-4$ and $V_2=1.571051$ with equal concentrations. CBE resonance located at $\epsilon_c=0.814459$. Notice that for the Lyapunov exponent the vertical scales are different before and after the resonance to ensure an optimal visualization. Solid lines correspond to fits according to expression (32) for $\lambda(\epsilon)$ and $g(\epsilon)\sim|\epsilon-\epsilon_c|^{-1/2}$. (b) $V_1=5$ and $V_2=7$ with different concentrations. Commuting-resonance located at $\epsilon_c=2.601$. Solid lines correspond to quadratic fits for $\lambda(\epsilon)$ and linear fits for DOS.

It all can be observed in Fig. 11(b). With the dependence described for $\lambda(\epsilon)$ and $g(\epsilon)$, it follows that in a finite system the number of states near the commuting critical energy with a localization length larger than the system size scales as $\sqrt{N}$, the same as for the CBE resonances. This scaling is exhibited by very different disordered models with isolated extended states in their spectra[2,51,52] and it might be a universal feature of isolated resonances in one-dimensional disordered systems. The DOS and the Lyapunov exponent seem to balance their functional dependence near the critical energies to ensure the $\sqrt{N}$ scaling.

The different characters of the two types of extended states described also manifest themselves in the way that transmission resonances appear close to the critical energies for finite chains. In the vicinity of the CBE resonances one finds the behavior shown in Fig. 12. As the length of the system increases, the states corresponding to transmission resonances, marked by a sharp decrease of the Lyapunov exponent, start approaching the exact value of ϵ_c [notice that for finite chains the Lyapunov exponent is obtained from the transmission of the system according to $\lambda=-(2N)^{-1}\ln T$]. The larger the system is the more the states squeeze together near the critical energy [Fig. 12(b)]. It may be surprising that the exact value ϵ_c is not a transmission resonance when the length of the chain is finite. This energy becomes a resonance only when the length of the system goes to infinity. The reason for this is clear: the nature of transmission resonances is absolutely determined by the boundary conditions. Therefore when one considers a finite length system, the resonances arise at the energy values for which the states can satisfy the proper scattering boundary conditions at the extremes of the system with a high value of the transmission, and one expects the fulfilling of the boundary conditions to depend on the length and on the sequence of the chain. Then, the appearance of transmission resonances in the spectrum of a finite disordered system is an agreement between two factors: the spatial extension of the state and the boundary conditions. The former determines the range of energies in which one could find high transmission efficiencies (i.e., a range with low values of the Lyapunov exponent and the IPR) and the latter establishes the precise values of the energies within this range where the resonances occur. Of course this effect only becomes apparent at a very small scale of energies. Inspecting the IPR around ϵ_c, one finds that for a small scale of energies the inverse participation ratio does not reproduce the behavior of the Lyapunov exponent, so that the transmission resonances cannot be correctly identified from this quantity. For the different lengths considered the IPR reaches its minimum value N^{-1} exactly at ϵ_c and for higher energies it shows higher values of the same order of magnitude [Fig. 12(a)]. The behavior of the IPR can be understood by observing the explicit form of the envelope of the electronic state at different energies. In Figs. 12(c) the envelope of the states at ϵ_c and at two energies with high transmission for the 1000-atom chain can be seen. The IPR gives us information about the spatial structure of the state, but since it is a normalized quantity it lacks any information about the amplitude of the state, which is essentially the transmission. Hence the IPR does not retain all the information about the boundary conditions. It can be observed how the state (c.1) is strictly more extended that (c.2) and (c.3) which have valleys with zero amplitude, therefore one expects the IPR in the first case to be smaller than for the other two cases. However, the amplitude for (c.1) is almost zero $[T=3.7\times10^{-7}]$ while for the other two energies the states live with a transmission coefficient noticeably higher. If the length of the system grows, the amplitude of the state for ϵ_c would increase so that for an infinite system the state would be perfectly flat with amplitude 1. As a summary, the IPR ignores everything concerning the value of the global amplitude of the state and although open boundary conditions are absolutely necessary to build the state correctly, the information of the transmission coefficient is not contained in the IPR, and this makes it useless for identifying the exact energies of transmission resonances of a finite system within very small ranges of energy. On the other hand, this fact means that the IPR retains the information of the thermodynamic limit and as can be seen in Fig. 12(a) the minimum value N^{-1} is reached independently of the length of the system at the energy ϵ_c, which we know to be an extended state in the thermodynamic limit. It seems that this behavior of the IPR is a fingerprint of the existence of a CBE resonance and, in principle, could be useful for identifying such states in other models by studying finite realizations of the systems. Finally, we have also studied the Lyapunov exponent and the IPR

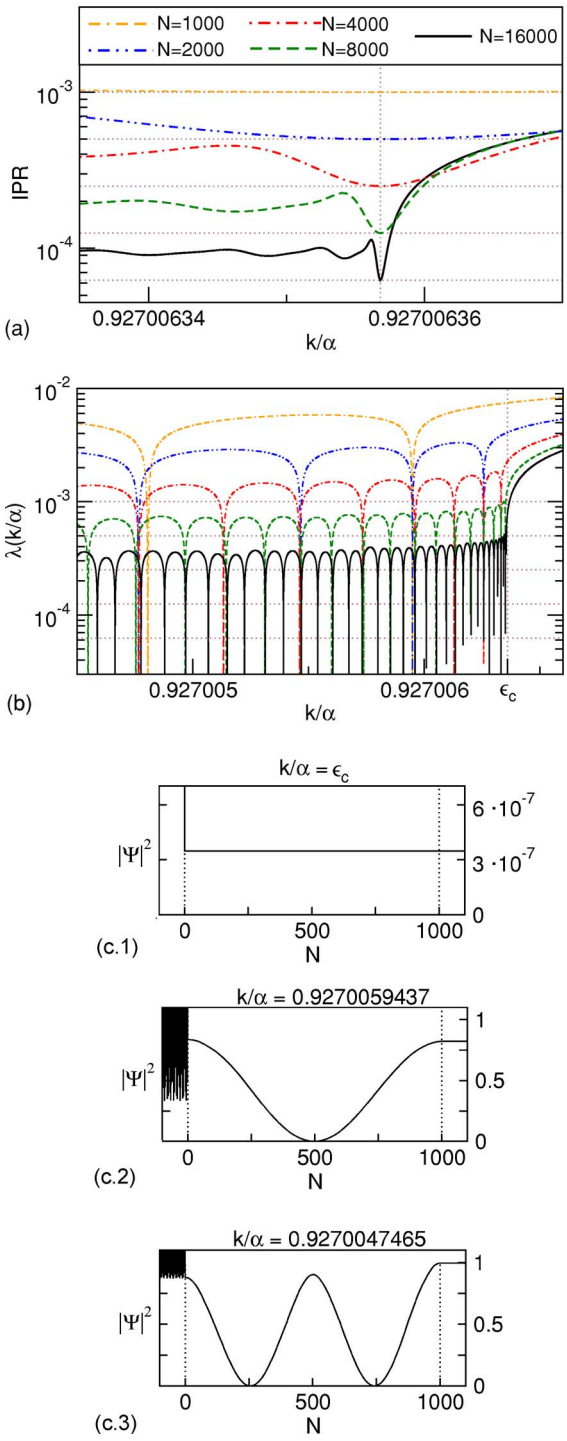

FIG. 12. (Color online) IPR (a) and Lyapunov exponent (b) near a CBE resonance for a binary chain with parameters $V_1=2$ and $V_2=-2.6422653344$ with equal concentrations. The critical energy is $\epsilon_c=0.9270063568$. The horizontal dotted lines mark the inverse of the length of the system in the different cases considered. Inside graphics (a) and (b) the length of the chain increases from top to bottom. For a given length, data of all graphics correspond to the same disordered sequence. Only one realization of the disorder has been considered for each length. Graphics at the bottom show the envelope of the electronic state for the chain with 1000 atoms for three different energies corresponding to transmissions (c.1) $T=3.7\times10^{-7}$, (c.2) $T=0.8207$, (c.3) $T=0.9955$.

averaging over several realizations of the disorder for a given finite length. And we are led to the conclusion that the behavior near the CBE resonances depends mainly on the length of the system and exhibits a weak dependence on the particular disordered sequence, since all the individual transmission matrices behaves essentially in a similar manner independently of the atomic species. After averaging, the hollows of the LE are slightly broadened in energy and shortened in height but they still appear at the same energies and the IPR shows the same aspect as for a single realization of the disorder. This confirms the fact that at this energy scale the IPR contains the information of the system in the thermodynamic limit. This strong dependence on the number of sites and not on the particular sequence explains why when the length of the system is increased proportionally, as in Fig. 12(b), the transmission resonances appear following a self-similar pattern.

Let us see what happens in the vicinity of a general commuting resonance. It is remarkable that the IPR for a finite system shows a characteristic plateau around the critical energy [Fig. 13(a)]. This flat zone gets narrower as the length of the system increases and it seems to be essentially symmetric around ϵ_c, which is in perfect agreement with the symmetric dependence of the Lyapunov exponent with the energy in this region in the thermodynamic limit. However in Fig. 13(a) it can be noticed that the IPR does not reach its minimum value N^{-1} for any energy. Nevertheless the inverse participation ratio for different lengths takes a value at ϵ_c that seems to scale roughly as $\mathrm{IPR}(\epsilon_c)\sim\frac{3}{2}N^{-1}$. Inspecting the Lyapunov exponent at a very small energetic scale near ϵ_c, it can be observed how as the length of the chain grows the number of transmission resonances increases following a symmetrical arrangement around the critical energy [Fig. 13(b)]. This is in great contrast to the CBE critical energies for which the transmission resonances are only located on one of the sides of ϵ_c. In Fig. 13(c) one can have a look at the appearance of the envelope of the electronic states with open boundary conditions near the critical energy for a chain with 1000 atoms. The states show a strongly fluctuating behaviour that seems to be modulated in a periodic manner. Apart from the differences in the global amplitude and the transmission, the three states shown exhibit essentially the same features. For the cases in Figs. 13—(c.2) and (c.3)—whose energy is not exactly the critical value, the periodic modulation starts to be subtly distorted. The spatial distribution of the states explains the behaviour of the IPR. First, all states near the critical energy have essentially the same structure leading to similar values of the IPR and therefore the plateau. And second, the fluctuating nature of the envelope of the states prevents the IPR from reaching its minimum value N^{-1}, which requires of the envelope of the state to be flat. In Fig. 14, one can observe how the state at the critical energy evolves as the concentration of the wire is changed for a finite binary system including 500 atoms. For pure one species chains the envelope shows a perfect periodic modulation, although the latter period sometimes can be larger than the size of the chain. The electronic state registers a morphing process through the disordered configurations between the two limiting pure cases and it always remains completely extended over the array. Let us also comment that within this small

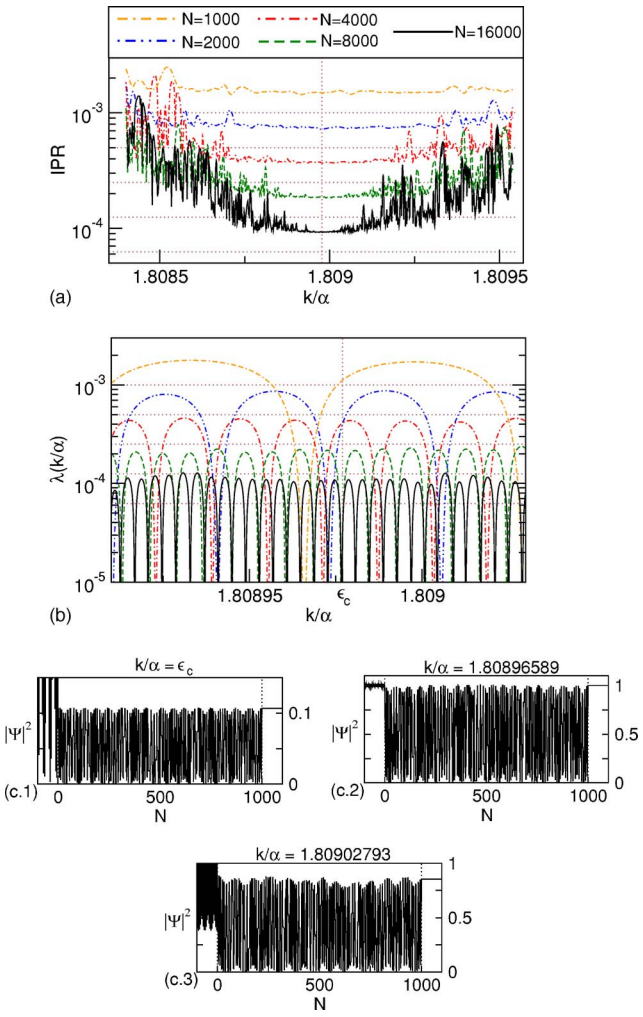

FIG. 13. (Color online) IPR (a) and Lyapunov exponent (b) near the critical energy $\epsilon_c=1.808977$ for a binary wire with parameters $V_1=-2.5$ and $V_2=5$ with equal concentrations. The horizontal dotted lines mark the inverse of the different lengths considered. Inside graphics (a) and (b) the length of the chain increases from top to bottom. For a given length, data of all graphics correspond to the same disordered sequence. Only one realization of the disorder has been considered for each length. Graphics at the bottom show the envelope of the electronic state for the chain with 1000 atoms for three different energies corresponding to transmissions (c.1) $T=0.1067$, (c.2) $T=0.9999$, (c.3) $T=0.8537$.

scale of energies near the commuting resonances, the influence of the atomic sequence is much more important than in the case of CBE resonances, because the structure of the envelope of the wave function at a local level is fully determined by the atomic sequence. Of course this dependence on the realization of the disorder gets weaker as the system grows. This influence can be noticed in Fig. 13(b), where the arrangement of the hollows of the Lyapunov exponent (i.e., resonances of the transmission) for different N seems more irregular than in the case of a CBE resonance (Fig. 12), although the length of the system is increased by the same factor in both cases. Only for the chain with 16 000 atoms the self-similar pattern in the appearance of transmission resonances emerges, manifesting that the effect of the length

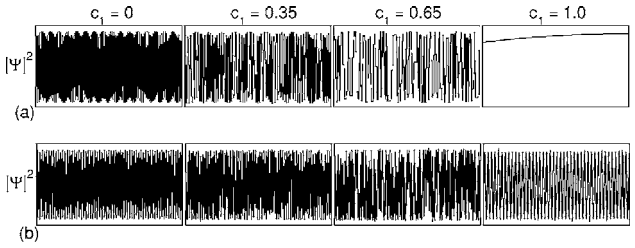

FIG. 14. Evolution of the envelope of the electronic state at a commuting critical energy as a function of concentration, for binary disordered wires with open boundary conditions. (a) $V_1=-2.5$, $V_2=5$ and $\epsilon_c=1.808977$, (b) $V_1=5$, $V_2=7$ and $\epsilon_c=2.600753$. In all cases the system includes 500 atoms and the states are properly normalized to make the comparison possible.

of the system has become stronger than the effect of the particular sequence.

Finally, we carried out the multifractal analysis for states near the commuting critical energies. This is somehow motivated by the fluctuating structure of the wave functions and also as an additional check of their real extended character. The multifractal analysis was first introduced to characterize the structure of a fractal distribution at various spatial scales via a set of generalized fractal dimensions.[53] The applicability of this tool to the study of electronic states comes from critical wave functions, which exhibit an intricate oscillatory behavior that may include self-similar fluctuations at different spatial scales (see Ref. 54 for a nice dissertation about critical states among many other things). Regarding electronic states, the multifractal analysis essentially studies the scaling of the different moments of the probability distribution of the state with the length of the system N. Those moments are defined as

$$\mu_q(N) \equiv \frac{\sum_j |\Psi_j|^{2q}}{\left(\sum_j |\Psi_j|^2\right)^q} \tag{33}$$

and the corresponding generalized fractal dimensions D_q are obtained from the scaling law $\mu_q(N) \sim N^{-(q-1)D_q}$ for large N. Let us notice that the second order moment μ_2 is the inverse participation ratio. The multifractal analysis is useful in order to decide on the localized or extended character of a given state, since one finds $D_q=0$ for all $q>1$ for a localized state whereas in the case of extended states, which spread over the whole system and show no fractal structure at all, D_q equals the spatial dimension of the system for all $q>1$. In Fig. 15 it can be seen for a binary wire that at the critical energy the moments considered scale with the length of the system according to $D_q=1$ confirming the extended character of the state, whereas for energies slightly deviated from the critical value the localized nature arises for a long enough system and the generalized fractal dimensions go to zero.

To close this subsection the summarized characteristics of the different types of extended states described can be found in Table I. Although those features correspond to the Pöschl-Teller model, we have studied that in the case of CBE resonances the delta model exhibits the same behavior,[45] there-

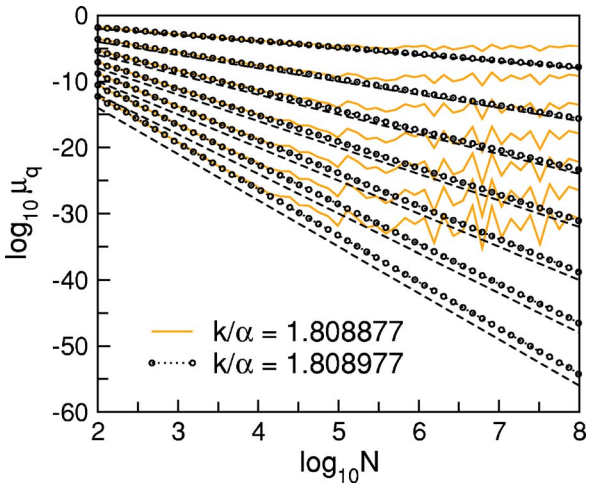

FIG. 15. (Color online) Multifractal analysis for a binary wire with parameters $V_1=-2.5$, $V_2=5$ with equal concentrations. The moments considered range from $q=2$ to $q=8$. Dashed lines correspond to equation $\mu_q(N)=N^{-(q-1)}$.

fore it would be very interesting to study whether the features of a given resonance (critical exponents, behavior of IPR, electronic envelope, etc.) are fully determined by the nature of the critical energy or on the contrary are also dependent upon the particular potential model.

C. Negative spectrum of the disordered wires

Let us have a look at the spectrum of bound states of the Pöschl-Teller wires. Most of the times the negative spectrum of disordered systems is not studied since it is not directly involved in the transport processes. The negative spectrum of our model exhibits interesting features very similar to those of the positive spectrum, that we shall briefly describe. One can wonder about the degree of localization of the electronic bound states. For negative energies the localization can still be characterized via the Lyapunov exponent even though its physical meaning cannot be defined in terms of the rate of decreasing of the transmission with the length of the system. The well defined meaning of the Lyapunov exponent for negative energies is guaranteed by Oseledet's multiplicative ergodic theorem (MET) (a complete analysis can be found in Ref. 55), as the quantity that measures the exponential divergence of an initial vector under the action of a product of random matrices. The continuous transmission matrices for negative energies are given in definition (5). The initial vector of amplitudes for the bound states must be $A_1=0, B_1=1$, where the amplitudes correspond respectively to the exponential solutions of the Schrödinger equation $e^{-\eta x}, e^{\eta x}$, where $\eta=\sqrt{2m|E|}/\hbar$. Then the MET implies that the Lyapunov exponent comes from

$$\lambda = \lim_{N\to\infty} \frac{1}{N} \ln \sqrt{\mathbb{M}_{12}^2 + \mathbb{M}_{22}^2}, \tag{34}$$

where $\mathbb{M}$ is the global matrix of the system. Since the final condition for a state to be bound is $\mathbb{M}_{22}=0$, one can equivalently characterize the electronic localization in a sufficiently large but finite system through

$$\lambda = \frac{1}{N} \ln|\mathbb{M}_{12}|. \tag{35}$$

Then the Lyapunov exponent for bound states can only be understood as a measure of the inverse of their localization length $\xi^{-1}(E)=\lambda(E)$ and the above definition is the natural extension for negative energies of the expression of the Lyapunov exponent in terms of the transmission coefficient for positive energies. On the other hand the Lyapunov exponent and the DOS for the negative spectrum of the wire in the thermodynamic limit can be straightforwardly obtained by using the functional equation formalism—which is valid for the whole spectrum—with the proper canonical functions given by Eqs. (14)–(16). Then one can speak of extended bound states whenever $\lambda=0$ and of exponentially localized bound states otherwise. From an academic viewpoint an extended bound state must be understood as an electronic state which decreases exponentially outside the system and that has essentially the same probability to be bound at any site of the chain. In other words, think of a bound state located at a given potential from which the state will decrease exponentially. Now imagine that this pattern repeats itself at every potential unit with a roughly constant amplitude, then we have an extended bound state. If on the contrary this pattern is only appreciable in a certain finite region of potential units then we can speak of a localized bound state.

TABLE I. Summary of features of the different types of isolated resonances in the spectrum of a disordered Pöschl-Teller wire.

Resonance	Critical Exponents	IPR	Envelope	States with $\lambda<N^{-1}$
Commuting	$\lambda\sim(\epsilon-\epsilon_c)^2$, $g(\epsilon)\sim g_0+(\epsilon-\epsilon_c)$	$\mathrm{IPR}(\epsilon_c)\neq N^{-1}$ plateau	Fluctuating	$\sqrt{N}$
CBE	$\lambda(\epsilon)\begin{cases}\lvert\epsilon-\epsilon_c\rvert^{1/2}\\ \lvert\epsilon-\epsilon_c\rvert\end{cases}$ $g(\epsilon)\begin{cases}0\\ \lvert\epsilon-\epsilon_c\rvert^{-1/2}\end{cases}$	$\mathrm{IPR}(\epsilon_c)=N^{-1}$	Flat	$\sqrt{N}$

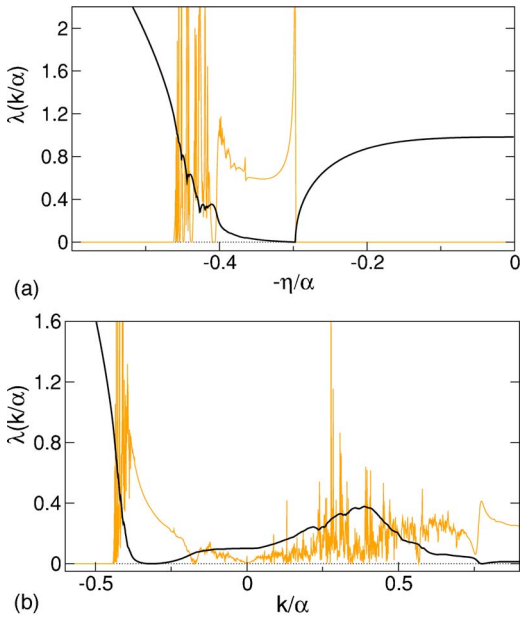

FIG. 16. (Color online) DOS and Lyapunov exponent (black) for binary chains. (a) $V_1=-0.5$, $V_2=-3.399309$ with equal concentrations. The CBE extended state occurs at $\epsilon_c=-0.297183$. (b) $\alpha_1=\alpha$, $V_1=-3.1$, $d_1^L=4.5/\alpha_1$, $d_1^R=4/\alpha_1$ and $\alpha_2=2\alpha$, $V_2=-2.5$, $d_2^L=5.5/\alpha_2$, $d_2^R=4.5/\alpha_2$ with equal concentrations. The commuting extended bound state is located at $\epsilon_c=-0.314670$. The negative part of the abscissa axis corresponds to $-\eta/\alpha$.

Extended bound states can generally be found using the same reasoning as for the positive spectrum. For example, imposing the condition $\Psi_{j+1}=\pm\Psi_j$ for all sites of the chain one can find the particular form the transmission matrices for negative energies must adopt to generate an extended state

$$\mathbf{M}=\begin{pmatrix}\pm 1-a(\eta) & -a(\eta)\\ a(\eta) & \pm 1+a(\eta)\end{pmatrix},\quad a(\eta)\in\mathbb{R}. \tag{36}$$

Imposing the proper equations to all species included in the chain one is led to the conclusion that this kind of extended bound states can only exist if all potential wells are symmetric ($d_j^R=d_j^L=d_j$), and in this case the following conditions must be satisfied:

$$q_j+\frac{1}{2}[f_j(-\eta)e^{-2\eta d_j}-f_j(\eta)e^{2\eta d_j}]=0,\quad \forall j, \tag{37}$$

in terms of q and $f(\eta)$ defined in Eqs. (6) and (7). And it readily follows from Eq. (36) that an energy satisfying these requirements is a common band-edge of the negative spectrum of the species. Therefore CBE extended bound states can be obtained, as one can see in Fig. 16(a).

Extended bound states can also exist at other type of commuting energies (not necessarily common band edges) that belong to the permitted spectrum of all species of the wire. For negative energies the commutator reads

$$[\mathbf{M}_1,\mathbf{M}_2]=\begin{pmatrix}F(-\eta) & H(\eta)\\ -H(-\eta) & F(\eta)\end{pmatrix}, \tag{38}$$

where

$$F(\eta)=2q_1q_2\sinh[\eta(d_1^L-d_2^L-d_1^R+d_2^R)], \tag{39}$$

$$H(\eta)=-e^{-\eta(d_2^R-d_2^L)}q_2[f_1(-\eta)e^{-\eta(d_1^L+d_1^R)}-f_1(\eta)e^{\eta(d_1^L+d_1^R)}]+e^{-\eta(d_1^R-d_1^L)}q_1[f_2(-\eta)e^{-\eta(d_2^L+d_2^R)}-f_2(\eta)e^{\eta(d_2^L+d_2^R)}]. \tag{40}$$

Commuting extended bound states can be found for a really wide range of the parameters of the potentials as long as the asymmetry of the species is the same $d_1^R-d_1^L=d_2^R-d_2^L$ since in this case $F(\eta)$ is identically zero and the only requirements to have a commuting energy are $H(\eta)=0$ and the condition of belonging to the permitted spectrum of both species, which can readily be obtained from the trace of the transmission matrix. An example is shown in Fig. 16(b).

A particular case that deserves a comment is the composition of wells for which b, defined in Eq. (3), is a half-integer (the case of integer b corresponds to the resonant well which will be treated in the next section). Let us remember that the dimensionless amplitude of the well can be written as $V=-b(b-1)$. We already know from Sec. II that the bound states of a well with a half-integer b correspond to half-integer values of η/α. It can easily be checked that the matrix of such a well at the eigenenergies reads

$$\mathbf{M}=\begin{pmatrix}0 & \pm e^{-\eta(d^R-d^L)}\\ \mp e^{\eta(d^R-d^L)} & 0\end{pmatrix}. \tag{41}$$

These matrices trivially commute with each other provided the asymmetry is the same for all wells. Therefore a chain including different wells with different half-integer values of b_γ and values for α_γ such that the potentials exhibit common levels will show extended bound states precisely at those energy levels, as can be seen in Fig. 17(a).

Even when b is not a half-integer, due to the structure of the discrete spectrum of the Pöschl-Teller (Fig. 2) is easy to choose a couple of different wells with common bound states, however, in this case the matrix of a general well for its eigenenergies reads

$$\mathbf{M}=\begin{pmatrix}f(-\eta)e^{-\eta(d^R+d^L)} & \pm e^{-\eta(d^R-d^L)}\\ \mp e^{\eta(d^R-d^L)} & 0\end{pmatrix} \tag{42}$$

and these matrices do not commute. Therefore the composition of wells with common bound states but with non half-integer (nor integer) values of b will not exhibit extended bound states at the common eigenenergies. Nevertheless since in this case all wells share common levels, a band of bound states is formed around these energies in the thermodynamic limit and we have checked that within these bands a commuting extended bound state always exists and it can be located quite near the common energy depending on the width of the band, as can be seen in Fig. 17(b). It must be emphasized that the behavior of λ and DOS around the different types of negative critical energies is the same as for their counterparts in the positive spectrum described in Table I.

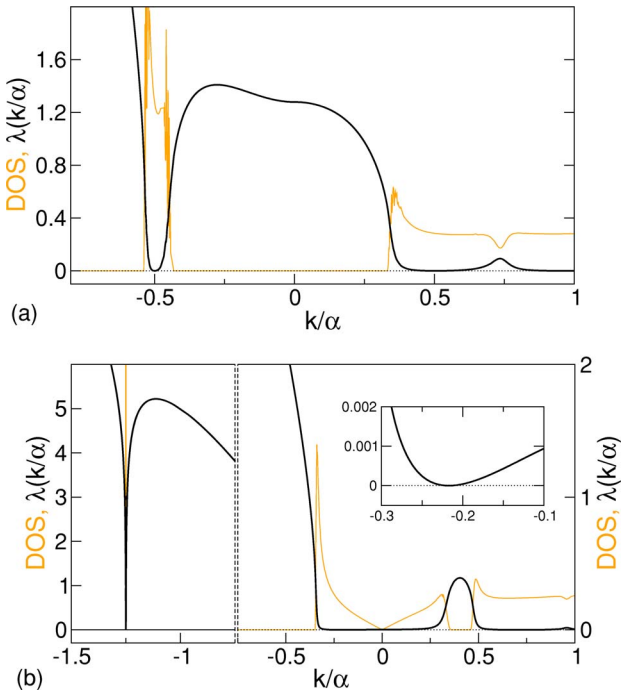

FIG. 17. (Color online) DOS and Lyapunov exponent (black) for binary chains including wells in equal concentrations with parameters (a) $b_1=3/2$, $b_2=5/2$ with a common eigenstate for $\eta/\alpha=0.5$ and (b) $V_1=-2.8125$ and $V_2=-7.3125$ showing common eigenstates at $\eta/\alpha=0.25, 1.25$. The commuting extended bound states are located at $\epsilon_c=-0.217142$ and $\epsilon_c=-1.25$. Notice the change in the vertical scale at −0.75 in the (b) example. The negative part of the abscissa axis represents $-\eta/\alpha$.

D. Including resonant wells in the disordered chain

Let us finally considered the interesting case of including resonant potential wells in the disordered system. The resonant wells correspond to potentials with an integer value of b greater than 1. From Sec. II we know that the transmission for this kind of potentials is identically 1 for all energies. The transmission matrix (9) for a resonant well for positive energies naturally reduces to

$$\mathbf{M} = \begin{pmatrix} e^{i[\varphi+k(d^L+d^R)]} & 0 \\ 0 & e^{-i[\varphi+k(d^L+d^R)]} \end{pmatrix}, \tag{43}$$

which is the transmission matrix of a zero potential. The resonant well for positive energies behaves as a zero potential with an effective length $L_{\text{eff}}(k)=\varphi/k+(d^R+d^L)$ that depends on the energy. This definition of the effective length only makes sense if it appears multiplied by the energy, since otherwise a divergence appears as k goes to zero. A handy expression can be obtained for the effective length. For a resonant well described by parameters $\{d_\gamma^L, d_\gamma^R, \alpha_\gamma, b_\gamma\}$ it can be proved by induction using the properties of the Gamma function that the following expression holds:

$$kL_{\text{eff}_\gamma}(k) \equiv \epsilon L_{\text{eff}_\gamma}(\epsilon) = \epsilon\frac{\alpha_\gamma d_\gamma^R + \alpha_\gamma d_\gamma^R}{(\alpha_\gamma/\alpha)} + (b_\gamma - 1)\pi - 2\sum_{j=1}^{b_\gamma-1} \arctan\left(\frac{\epsilon}{j(\alpha_\gamma/\alpha)}\right), \tag{44}$$

where $\epsilon \equiv k/\alpha$ and α being the reference value for the parameters $\{\alpha_\gamma\}$. Let us briefly analyse the appearance of critical energies for a binary chain in which one of the potentials is a resonant well. Since for the resonant well $w_\gamma=0$ the conditions of positive commuting resonance reduce simply to

$$\sin[kL_{\text{eff}_\gamma}(k)] = 0, \tag{45}$$

plus the condition of belonging to the permitted spectrum of the other species and without further restrictions on the parameters of the second potential. In the case of CBE resonances, since the resonant well has no gaps in its positive spectrum it can easily be checked that the conditions (30) reduce also to Eq. (45) together with the energy being an appropriate band-edge of the spectrum of the second species. Therefore in a binary chain with one of the species being a resonant well, transmission resonances can only lie among the set of energies satisfying $\epsilon L_{\text{eff}_\gamma}(\epsilon)=n\pi$, $n \in \mathbb{Z}$. For the negative spectrum one similarly obtains that extended bound states must fulfill the equation

$$e^{-\eta(d_\gamma^L+d_\gamma^R)} f_\gamma(-\eta) - e^{\eta(d_\gamma^L+d_\gamma^R)} f_\gamma(\eta) = 0, \tag{46}$$

where $f_\gamma(\eta)$ for a resonant well can be expressed as

$$f_\gamma(\eta) = \prod_{j=1}^{b_\gamma-1} \frac{\eta/\alpha_\gamma - j}{\eta/\alpha_\gamma + j}. \tag{47}$$

If such an energy lies in the permitted spectrum of the other species then a commuting extended bound state emerges without further requirements on the parameters of the second species. On the other hand if the energy coincides with a band edge of the negative spectrum of the second species, which must be a symmetric well, then we have a CBE extended bound state.

Now let us consider a disordered chain entirely composed of different resonant wells. Regarding the negative spectrum of the chain, the matrix of a resonant well for its eigenlevels is the same as for the case of half-integer b discussed previously [Eq. (41)]. Let us remember that the well host $(b_\gamma - 1)$ bound states that correspond to integer values of η/α_γ. Therefore the common eigenlevels of all resonant wells, according to parameters $\{\alpha_\gamma\}$, will arise as extended bound states as long as the asymmetry of all wells is the same. For positive energies, the disordered chain composed of different resonant wells behaves as a transparent potential for all energies: the canonical equation reduces to the canonical equation for the free particle so the system exhibits a maximum transmission. The properties of these resonant chains have been analyzed in detail by the authors in Ref. 39, where the analytical expression for the DOS is obtained and the tolerance of the transmission with the parameters of the potential

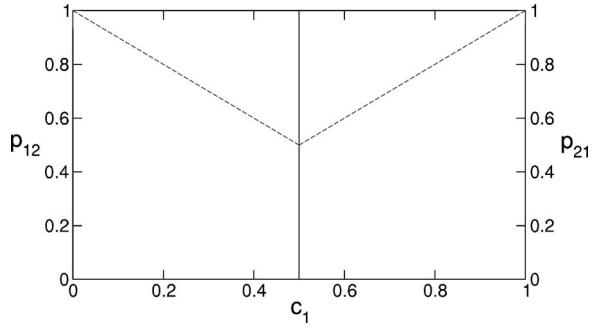

FIG. 18. Optimal representation of the correlation space for two species as a function of the concentration: if $c_1 \leqslant 0.5$ then p_{12} vs c_1, if $c_1 > 0.5$ then p_{21} vs c_1. The dashed line corresponds to the completely random configurations.

as well as the influence of the approximations made to build the matrix of the Pöschl-Teller potential are discussed.

V. WIRES WITH CORRELATED SUBSTITUTIONAL DISORDER

The Pöschl-Teller potential model can be also studied under the effect of correlated substitutional disorder. The model of short-range correlations proposed has been also applied successfully by the authors to the delta potential system, and it is thoroughly described in Refs. 3, 4, and 45. We shall make here only a brief description. In the completely random case, the properties of the system are determined by the parameters of the different atomic species composing the chain and their concentrations $\{c_\gamma\}$. One can introduce short-range correlations in the structure modifying the probability of different atomic clusters to appear in the wire sequence. This can be done by considering an additional set of probabilities $\{p_{\gamma\beta}\}$ obeying certain equations, where $p_{\gamma\beta}$ means the probability for a γ atom to be followed or preceded by a β atom. Thus the frequency of appearance of binary atomic clusters can be altered by these quantities. The probability of finding at any position the couple $-\gamma\beta-(-\beta\gamma-)$ would be $c_\gamma p_{\gamma\beta}$ or equivalently $c_\beta p_{\beta\gamma}$. Then in the thermodynamic limit the physical properties of such a system will depend upon the parameters of the species, the concentrations, and the probabilities $\{p_{\gamma\beta}\}$. This correlated model naturally includes the situation when the disorder in the wire is completely random, that is just defined by the values $p_{\gamma\beta}=c_\beta$. In this section only binary chains will be considered, so let us study in detail the correlation scheme for this case. Our wire will be determined by one of the concentrations $\{c_1,c_2\}$ and one of the probabilities $\{p_{11},p_{12},p_{21},p_{22}\}$, that satisfy the relations $p_{11}+p_{12}=p_{22}+p_{21}=1$ and $c_1p_{12}=c_2p_{21}$. One usually takes as configuration parameters $c_1 \leqslant 1$ and $p_{12} \leqslant \min\{1,c_2/c_1\}$. However, one can optimize the representation of this configurational space by choosing the parameters $\{c_1,p_{12}\}$ when $c_1 \leqslant 0.5$ and $\{c_1,p_{21}\}$ when $c_1 > 0.5$, so that the configuration space is expanded and the spatial points can be better differentiated, as shown in Fig. 18. Therefore, for a given concentration different values for $p_{12}(p_{21})$ can be chosen, and only one of them corresponds to the completely random chain. When the configuration of the binary chain lies on the dashed lines of Fig. 18, we have a completely random chain whereas if the configuration lies anywhere else we have a correlated chain.

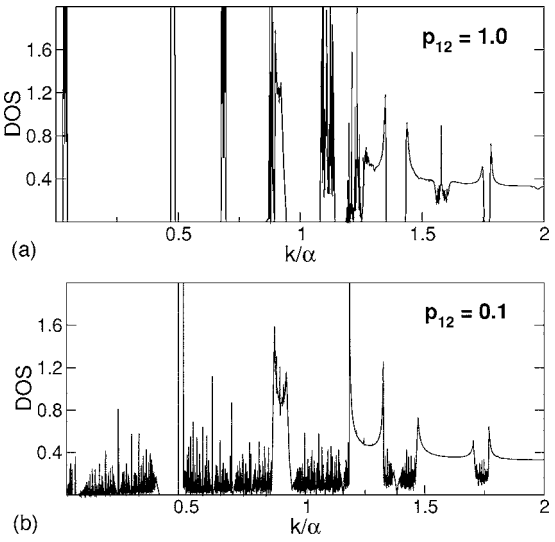

FIG. 19. DOS for correlated configurations of a binary chain with parameters $V_1=-2.5$ and $V_2=2$ with concentration $c_1=0.4$.

A. Effects of the correlations in the thermodynamic limit

The limiting distributions of the DOS and the Lyapunov exponent for the infinite system can be obtained numerically using the functional equation formalism which in its more general form accounts for the presence of correlations through the probabilities $\{p_{\gamma\beta}\}$.[44,45] The density of states of a binary chain is altered by the effect of the correlations in a similar manner as for the delta model.[3] In Fig. 19 the DOS is plotted for two limiting correlated situations of a binary chain with fixed concentrations. The distribution of states changes from the initial situation in which the probability to find the cluster –12– is low ($p_{12}=0.1$), to the stage when the atoms of species 1 appear always isolated ($p_{12}=1.0$). The number of available states in certain ranges as well as the gaps can be changed by tuning p_{12}, although the concentrations remain fixed. It can also be checked that for the correlated configurations the fractal character of the distribution persists in different energy intervals.

The effect of the correlations on the electronic localization is also similar as for the delta model. The Lyapunov exponent is globally altered by the correlations in the whole energy spectrum, although as expected no new extended states emerge in the thermodynamic limit, as can be seen in the examples of Fig. 20. The evolution of the Lyapunov exponent for a fixed concentration with the probability p_{12} agrees perfectly with the behavior of the inverse participation ratio calculated by averaging over many finite realizations of the disordered system. Let us note that the critical energies of the spectrum corresponding to extended states are present in all the different correlated regimes. It is also remarkable the fact that as the correlations change, the value of the Lyapunov exponent can be strongly decreased for several energies. These energies for which the localization can be

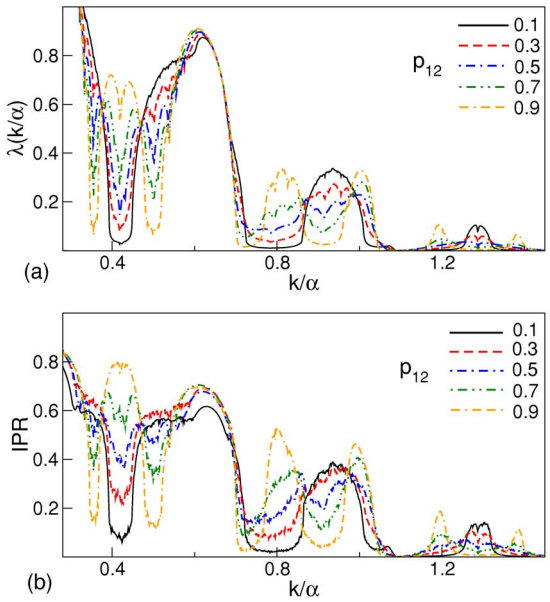

FIG. 20. (Color online) Evolution of the Lyapunov exponent (a) and the IPR (b) with the correlations for a binary chain with parameters $V_1=-1$, $V_2=1$, $c_1=0.5$. Notice the presence of a critical energy at $\epsilon_c=1.095$. For each configuration the IPR has been obtained by averaging 100 sequences of a 1000-atom array.

severely weakened are related to resonances of different atomic clusters whose concentration is modified by the correlations. For example, in a binary chain composed of a well (1) and a barrier (2), for the case $p_{12}=1.0$ the wells are completely isolated so that they always appear in the cluster barrier-well-barrier. Therefore it seems reasonable that in this correlated situation the energies of transmission resonances of the latter cluster will tend to be more delocalized than for any other value of p_{12}. This effect is more noticeable in this model than for the delta model, since in that case the atomic potentials lack an internal structure. We have also checked that the effect of the correlations is similar when more species are included in the disordered wire.

B. Effects of the correlations on finite wires

Although not truly extended states are included in the spectrum, the effects of these short-range correlations upon finite samples of the wires are able to improve noticeably the electronic transport, much the same way as for the delta model.[4] In Fig. 21 several transmission patterns for a finite binary chain composed of 1000 atoms are plotted. In the correlated configurations the transmission is improved with respect to the completely random situation. Let us notice that the improvement can take place in different energy ranges and it is not restricted to the vicinity of the critical energies. As expected, the enhancement of transmission occurs in the whole configurational space of the binary wire as revealed by the transmission efficiency

$$T_{\text{eff}} = \frac{1}{k_2 - k_1} \int_{k_1}^{k_2} T(k) dk. \tag{48}$$

The minimum intensity of the transport is found around the completely random lines whereas the correlated configurations perform always better (Fig. 22). The patterns of the enhancement are similar to those of the δ model although it must be emphasized that the transmission efficiency may adopt a strong asymmetric distribution over the configuration space, depending on the species amplitudes. This asymmetry is absolutely negligible in the δ model since the δ potential from the point of view of the transmission behaves essentially in the same way independently of the sign of the coupling. However provided the atomic potentials are nonpunctual and have an internal structure, this asymmetry may be quite noticeable since a potential well performs a better transmission than a potential barrier, and the same thing happens comparing barriers of different heights. Therefore the transmission efficiency naturally registers a global lift or a global decrease depending on whether the concentration of the species that is more tolerant with the transmission process is larger or less than 0.5.

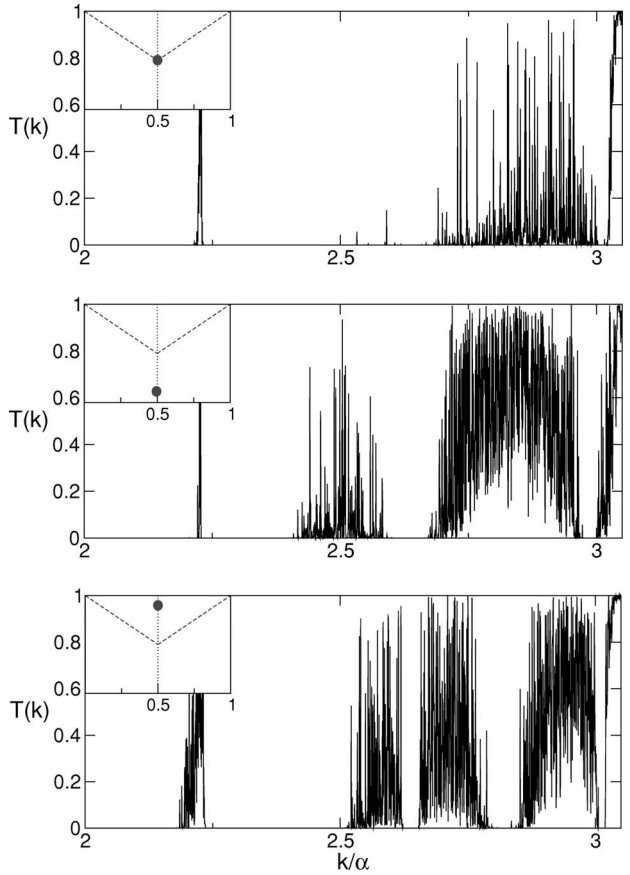

FIG. 21. Transmission probability vs energy for a 1000-atom binary disordered chain in different correlation regimes. The circular point inside the insets marks the configuration on the configurational space. Only one realization of the disorder has been considered for each case. Parameters: $V_1=-2.5$, $V_2=5$, $c_1=0.5$ and correlation from top to bottom $p_{12}=0.5, 0.1, 0.9$.

Then the enhancement of transmission in finite wires is a fact. And the reason is that the short-range correlations modify the localization in the thermodynamic limit in such a way that the fluctuations of the Lyapunov exponent for a finite system cause an important increase of the number of states whose localization length (ξ) is larger than the system

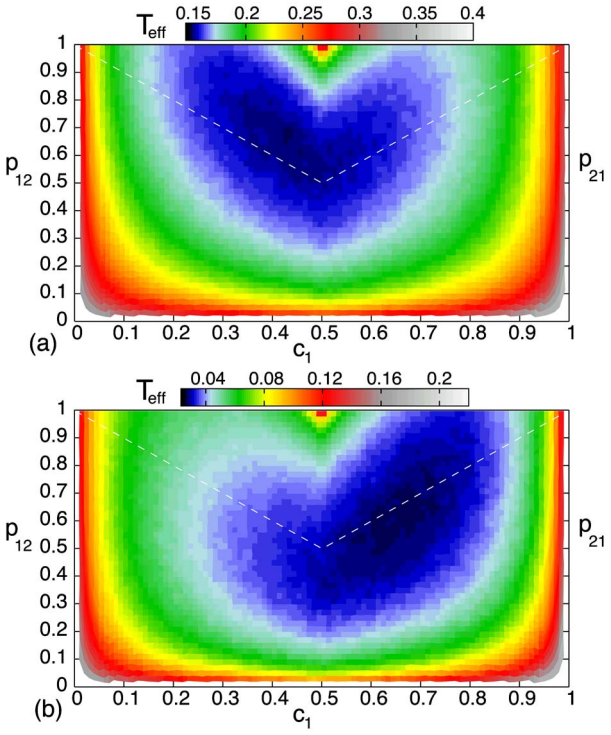

FIG. 22. (Color online) Transmission efficiency over correlation space for binary chains: (a) $V_1=-2.5$, $V_2=5$ and integration interval [0, 3.7], (b) $V_1=2.5$, $V_2=5$ and integration interval [0, 3].

size (N). This seems to be a universal effect of this sort of correlations independently of the atomic model. Additionally, once the compositional species and the concentrations of the wire are fixed, the correlations can be chosen to localize to a certain extent the improvement of transmission in a particular energy range.

As the length of the wire grows the effects of the correlations disappear; the completely random chain displays the fastest decay of T_{eff} with the size of the system whereas the correlated situations show higher efficiencies for all lengths, as can be seen in Fig. 23. The relative differences $\Delta T_{\text{eff}} = T_{\text{eff}} - T_{\text{eff}}(R)$ as a function of the length, where (R) means the completely random value, reveals that the effect of the correlations is generally maximized for short chains. From the analysis made on the Pöschl-Teller wires and the delta wires, it must be remarked that the effects described of this type of correlated disorder are essentially independent of the potential model.

VI. FINAL DISCUSSION

In this chapter the Pöschl-Teller potential has been considered to build one-dimensional quantum wires. The properties of the whole spectrum (positive and negative energies) of the disordered wire in the thermodynamic limit have been thoroughly studied using the canonical equation and the functional equation formalism.

Fractality in certain energy ranges of the density of states has manifested itself as a property of the spectra of these disordered systems, and it seems to be a characteristic feature

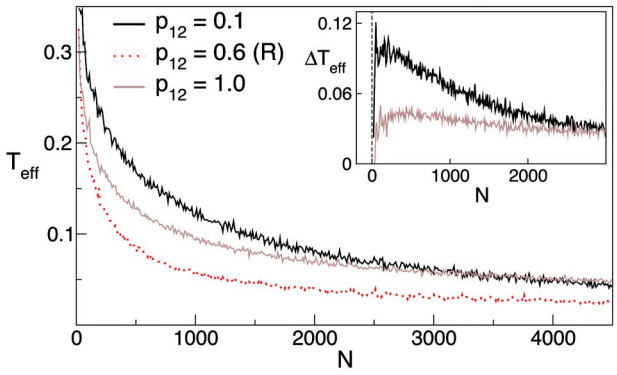

FIG. 23. (Color online) Transmission efficiency vs length for different configurations of a 1000-atom binary chain with parameters $V_1=-1$, $V_2=1$, $c_1=0.4$, integration interval [0, 1.75]. (R) marks the completely random situation. The inset shows the relative differences $\Delta T_{\text{eff}}=T_{\text{eff}}-T_{\text{eff}}(R)$.

of one-dimensional disordered systems independently of the potential model. Its relation with localization and its dependence upon the nature of the distributions that define the disorder is currently under investigation.

The analysis of localization has also revealed the existence of two types of isolated extended states: CBE resonances and commuting resonances, exhibiting very dissimilar characteristics: different critical exponents for λ and DOS, different behavior of the IPR and different aspect of the envelope of the state. However, they share some common features, such as the fact that the number of states near the resonance with a localization length larger than the system size scales as the square root of the length of the chain. One can wonder whether the properties of such critical energies are dependent upon the particular potential model considered to build the disordered chain or on the contrary Table I means a universal classification scheme. As we already know the features of the delta potential model also fits in the given table.[45] But the most interesting thing is that all extended states found are located at commuting energies, ensuring the commutativity of the transmission matrices composing the array. Then one can conjecture that all extended states in 1D systems may be located at commuting-energies of the spectrum. As we have seen, this common origin is compatible with very different features of the extended states, and if it were true it would mean to have a very simple condition to find all possible resonances that can occur in a one-dimensional disordered system. Of course, we must not forget that the additional condition of belonging to the permitted spectrum of all species of the chain has also to be satisfied by the commuting energy. In order to support this conjecture let us see that even when short-range correlations are included in the disorder, the extended states occur at commuting energies. Let us consider, for example, the famous binary random-dimer model. One of the atomic species appears always in pairs (dimers), then in general the matrix of the dimer reads

$$\begin{pmatrix} \alpha & \beta \\ \beta^* & \alpha^* \end{pmatrix}\begin{pmatrix} \alpha & \beta \\ \beta^* & \alpha^* \end{pmatrix} = \begin{pmatrix} \alpha^2 + |\alpha|^2 - 1 & 2\beta\,\mathrm{Re}(\alpha) \\ 2\beta^*\,\mathrm{Re}(\alpha) & (\alpha^*)^2 + |\alpha|^2 - 1 \end{pmatrix}, \tag{49}$$

where we have used $|\alpha|^2 - |\beta|^2 = 1$. Then, due to the dimeric structure of the matrix it is possible that new resonant states emerge in the spectrum at energies for which the dimer matrix commutes with the matrix of the other species. The simplest case corresponds to the situation when the dimer matrix reduces to a multiple of the identity matrix, and that occurs whenever $\mathrm{Re}(\alpha) = 0$ as can be seen in the above expression. Then the only left condition to have a resonance is that the energy belongs to the permitted spectrum of the nondimerized species. This is the most simple way to write the condition of the dimer resonance and it is independent of the potential model. Moreover, other commuting energies can exist for which the dimer matrix does not reduce to the identity, since it suffices that the dimer matrix ($\mathbf{M}_{\mathrm{dimer}}$) can be written as a combination of the identity and powers of the matrix of the nondimerized species ($\bar{\mathbf{M}}$),

$$\mathbf{M}_{\mathrm{dimer}} = a_0\mathbf{I} + \sum_{n>0} a_n \bar{\mathbf{M}}^n. \tag{50}$$

The same reasoning can also be applied to other types of impurities that can be included inside a periodic chain. In fact, it has been found that if the impurities are symmetric then extended states can exist at energies for which the impurity matrix reduces to a linear combination of the identity and the matrix of the other species of the chain,[5,56] hence they are commuting resonances. Therefore, this kind of short-range correlations are able to include new extended states in the spectrum because there exist energies for which the matrices of the new compositional units (i.e., the dimer matrix or the impurity matrix and the matrices of the other species) can commute. Some of these commuting energies will not be commuting energies of the individual matrices of the system and that is the reason why these extended states do not exist in the uncorrelated model. Let us consider another correlated model supporting extended states, for example the simplest case of the diluted Anderson model.[6,52] It consists of a one-dimensional tight-binding Hamiltonian for which the self-energies ε_j of the odd sites are random, whereas they are all equal for the even sites that can be set to zero without loss of generality. This model is known to support an extended state for $E=0$. Let us see that it is a commuting resonance. The discrete transfer matrix (i.e., the matrix defined from the canonical equation) for the diagonal tight-binding model reads

$$\mathbf{P}_j = \begin{pmatrix} E - \varepsilon_j & -1 \\ 1 & 0 \end{pmatrix}. \tag{51}$$

We can define a new compositional unit in the system including an odd and an even site, which can be described by the product of the individual matrices

$$\mathbf{M}_j = \begin{pmatrix} E^2 - \varepsilon_j E - 1 & \varepsilon_j - E \\ E & -1 \end{pmatrix} \tag{52}$$

and the commutator of these compositional units can be readily calculated

$$[\mathbf{M}_j, \mathbf{M}_i] = \begin{pmatrix} (\varepsilon_j - \varepsilon_i)E & 0 \\ (\varepsilon_j - \varepsilon_i)E^2 & (\varepsilon_i - \varepsilon_j)E \end{pmatrix}, \tag{53}$$

that obviously vanishes for $E=0$ independently of the values of the site energies. It can be easily seen that $E=0$ belongs to the permitted spectrum of the periodic chain of matrices (52) for all values of ε_j, and therefore a commuting-resonance emerges at that energy whatever the distribution of the site energies for the odd sites is. It can be shown that the extended states appearing in more complex configurations of the diluted Anderson model are also commuting resonances. It must then be clear that not all kind of short-range correlations will be able to include new extended states in the spectrum in the thermodynamic limit. The correlations must be such that new compositional units can be defined in the system, so that new commuting energies for the matrices of the new compositional units can exist. This reasoning explains why the model of correlations proposed in this work is not able to include new extended states, since the probability of appearance of certain binary clusters is modified but the compositional units of the system remain the same as for the completely random case, and they are the individual matrices of the atomic species. Then, although the localization and the transport properties can be modified by the correlations, as it has been shown, however, no additional truly extended states emerge in the spectrum. And, what about long-range correlations? Certainly the situation is quite more complex with long-range correlations, however, at the present time, to our knowledge, there does not exist in the literature any proof that long-range correlations are able to include in the spectrum of disordered systems strictly extended states, that is with a divergent localization length. Only numerical proofs[15,16,57] and also analytical calculations up to fourth order in perturbation theory[17–19] exist that have proved that qualitatively a MIT happens due to long-range correlations, and it has been experimentally checked.[23,24] However, the states of the "delocalized" phase are strictly speaking still exponentially localized. Hence, it seems that a large variety of models existing so far in the literature are compatible with the conjecture that all extended states in the thermodynamic limit of one-dimensional disordered structures occur at commuting energies of the transmission matrices of the compositional units of the system. Nevertheless, further research is needed to confirm the validity of such a hypothesis.

Among all the interesting features exhibited by the Pöschl-Teller model, such as the presence of isolated extended states in uncorrelated disordered sequences in which the parameters of the different species satisfy certain properties, one of them deserves a special remark: the building of random resonant chains with a continuum of delocalized states. The composition of resonant Pöschl-Teller wells behaves as a transparent potential for all positive energies, as described in detail in Ref. 39.

Finally, the analysis of a model of short-range correlations previously studied by the authors in other potentials, has revealed that the physical effects of this type of correlated disorder are the same independently of the potential model. The correlations are able to alter the distribution of states and the localization length globally in the thermodynamic limit although no new critical energies occur. Nevertheless for a finite system the number of states with a localization length larger than the system size increases dramatically in the correlated configurations with respect to the completely random situation, thus yielding a noticeable improvement of the transmission efficiency for the correlated disordered sequences.

The disordered Pöschl-Teller chains show an ensemble of very interesting properties and also an unexpected behavior not anticipated from a disordered system. From our point of view, it is important to build new models of one-dimensional disordered systems using other potentials, in order to analyze their properties and decide on the validity of our conjectures.

ACKNOWLEDGMENTS

This research has been partially supported by DGICYT under Contracts Nos. BFM2002-02609 and FIS2005-01375.

*Electronic address: argon@usal.es

[1] P. W. Anderson, Phys. Rev. **109**, 1492 (1958).
[2] A. Sánchez, E. Maciá, and F. Domínguez-Adame, Phys. Rev. B **49**, 147 (1994).
[3] J. M. Cerveró and A. Rodríguez, Eur. Phys. J. B **32**, 537 (2003).
[4] J. M. Cerveró and A. Rodríguez, Eur. Phys. J. B **43**, 543 (2005).
[5] H. L. Wu, W. Goff, and P. Phillips, Phys. Rev. B **45**, 1623 (1992).
[6] M. Hilke, J. Phys. A **30**, L367 (1997).
[7] J. C. Flores, J. Phys.: Condens. Matter **1**, 8471 (1989).
[8] D. H. Dunlap, H.-L. Wu, and P. W. Phillips, Phys. Rev. Lett. **65**, 88 (1990).
[9] J. C. Flores and M. Hilke, J. Phys. A **26**, L1255 (1993).
[10] F. M. Izrailev, T. Kottos, and G. P. Tsironis, J. Phys.: Condens. Matter **8**, 2823 (1996).
[11] E. Diez, A. Sánchez, and F. Domínguez-Adame, Phys. Rev. B **50**, 14359 (1994).
[12] T. Sedrakyan, Phys. Rev. B **69**, 085109 (2004).
[13] W. Zhang and S. E. Ulloa, Phys. Rev. B **69**, 153203 (2004).
[14] F. A. B. F. de Moura, M. N. B. Santos, U. L. Fulco, M. L. Lyra, E. Lazo, and M. E. Onell, Eur. Phys. J. B **36**, 81 (2003).
[15] F. A. B. F. de Moura and M. L. Lyra, Phys. Rev. Lett. **81**, 3735 (1998).
[16] H. Shima, T. Nomura, and T. Nakayama, Phys. Rev. B **70**, 075116 (2004).
[17] F. M. Izrailev and A. A. Krokhin, Phys. Rev. Lett. **82**, 4062 (1999).
[18] F. M. Izrailev, A. A. Krokhin, and S. E. Ulloa, Phys. Rev. B **63**, 041102(R) (2001).
[19] L. Tessieri, J. Phys. A **35**, 9585 (2002).
[20] F. A. B. F. de Moura and M. L. Lyra, Physica A **266**, 465 (1999).
[21] F. M. Izrailev and N. M. Makarov, J. Phys. A **38**, 10613 (2005).
[22] V. Bellani, E. Diez, R. Hey, L. Toni, L. Tarricone, G. B. Parravicini, F. Domínguez-Adame, and R. Gómez-Alcalá, Phys. Rev. Lett. **82**, 2159 (1999).
[23] A. Krokhin, F. Izrailev, U. Kuhl, H. J. Stöckmann, and S. E. Ulloa, Physica E (Amsterdam) **13**, 695 (2002).
[24] U. Kuhl, F. Izrailev, A. Krokhin, and H. J. Stöckmann, Appl. Phys. Lett. **77**, 633 (2000).
[25] F. Domínguez-Adame, V. A. Malyshev, F. A. B. F. de Moura, and M. L. Lyra, Phys. Rev. Lett. **91**, 197402 (2003).
[26] F. A. B. F. de Moura, M. L. Lyra, F. Domínguez-Adame, and V. A. Malyshev, Phys. Rev. B **71**, 104303 (2005).
[27] A. Rodríguez, V. A. Malyshev, G. Sierra, M. A. Martín-Delgado, J. Rodríguez-Laguna, and F. Domínguez-Adame, Phys. Rev. Lett. **90**, 027404 (2003).
[28] A. V. Malyshev, V. A. Malyshev, and F. Domínguez-Adame, Phys. Rev. B **70**, 172202 (2004).
[29] F. A. B. F. de Moura, A. V. Malyshev, M. L. Lyra, V. A. Malyshev, and F. Domínguez-Adame, Phys. Rev. B **71**, 174203 (2005).
[30] P. A. Lee and T. V. Ramakrishnan, Rev. Mod. Phys. **57**, 287 (1985).
[31] L. I. Deych, M. V. Erementchouk, and A. A. Lisyansky, Phys. Rev. Lett. **90**, 126601 (2003).
[32] L. I. Deych, A. A. Lisyansky, and B. L. Altshuler, Phys. Rev. Lett. **84**, 2678 (2000).
[33] L. I. Deych, M. V. Erementchouk, and A. A. Lisyansky, Phys. Rev. B **67**, 024205 (2003).
[34] T. Schulte, S. Drenkelforth, J. Kruse, W. Ertmer, J. Arlt, K. Sacha, J. Zakrzewski, and M. Lewenstein, Phys. Rev. Lett. **95**, 170411 (2005).
[35] J. E. Lye, L. Fallani, M. Modugno, D. S. Wiersma, C. Fort, and M. Inguscio, Phys. Rev. Lett. **95**, 070401 (2005).
[36] B. Damski, J. Zakrzewski, L. Santos, P. Zoller, and M. Lewenstein, Phys. Rev. Lett. **91**, 080403 (2003).
[37] H. Gimperlein, S. Wessel, J. Schmiedmayer, and L. Santos, Phys. Rev. Lett. **95**, 170401 (2005).
[38] U. Gavish and Y. Castin, Phys. Rev. Lett. **95**, 020401 (2005).
[39] A. Rodríguez and J. M. Cerveró, Phys. Rev. B **72**, 193312 (2005).
[40] S. Flügge, *Practical Quantum Mechanics* (Springer-Verlag, Berlin, 1970).
[41] A. Khare and U. P. Sukhatme, J. Phys. A **21**, L501 (1988).
[42] J. W. Dabrowska, A. Khare, and U. P. Sukhatme, J. Phys. A **21**, L195 (1988).
[43] J. M Cerveró and A. Rodríguez, Phys. Rev. A **70**, 052705 (2004).
[44] A. Rodríguez, quant-ph/0603133 (unpublished).
[45] A. Rodríguez, Ph.D. thesis, Universidad de Salamanca, Salamanca, 2005, http://www.usal.es/fnl/argon/downloads/Thesis.pdf
[46] J. M Cerveró and A. Rodríguez, Eur. Phys. J. B **30**, 239 (2002).
[47] A. Rodríguez and J. M. Cerveró (unpublished).
[48] I. Gómez, F. Domínguez-Adame, and E. Diez, Physica B **324**, 235 (2002).

[49] M. Hilke and J. C. Flores, Phys. Rev. B **55**, 10625 (1997).
[50] M. Y. Azbel, Phys. Rev. B **28**, 4106 (1983).
[51] A. Bovier, J. Phys. A **25**, 1021 (1992).
[52] F. Domínguez-Adame, I. Gómez, A. Avakyan, D. Sedrakyan, and A. Sedrakyan, Phys. Status Solidi B **221**, 633 (2000).
[53] T. C. Halsey, M. H. Jensen, L. P. Kadanoff, I. Procaccia, and B. I. Shraiman, Phys. Rev. A **33**, 1141 (1986).
[54] E. Maciá and F. Domínguez-Adame, *Electrons, Phonons and Excitons in Low Dimensional Aperiodic Systems* (Editorial Complutense, Madrid, 2000).
[55] L. Arnold, *Random Dynamical Systems* (Springer Verlag, Berlin, 1998).
[56] X. Q. Huang, R. W. Peng, F. Qiu, S. S. Jiang, and A. Hu, Eur. Phys. J. B **23**, 275 (2001).
[57] S. Russ, J. W. Kantelhardt, A. Bunde, and S. Havlin, Phys. Rev. B **64**, 134209 (2001).